REVIEW ARTICLE

A review of normal tissue hydrogen NMR relaxation times and relaxation mechanisms from 1–100 MHz: Dependence on tissue type, NMR frequency, temperature, species, excision, and age

Paul A. Bottomley, Thomas H. Foster, Raymond E. Argersinger, and Leah M. Pfeifer

General Electric Corporate Research and Development Center, Schenectady, New York 12301

(Received 9 February 1984; accepted for publication 4 May 1984)

The longitudinal (T_1) and transverse (T_2) hydrogen (^{1}H) nuclear magnetic resonance (NMR) relaxation times of normal human and animal tissue in the frequency range 1–100 MHz are compiled and reviewed as a function of tissue type, NMR frequency, temperature, species, *in vivo* versus *in vitro* status, time after excision, and age. The dominant observed factors affecting T_1 are tissue type and NMR frequency (ν). All tissue frequency dispersions can be fitted to the simple expression $T_1 = A\nu^B$ in the range 1–100 MHz, with A and B tissue-dependent constants. This equation provides as good or better fit to the data as previous more complex formulas. T_2 is found to be multicomponent, essentially independent of NMR frequency, and dependent mainly on tissue type. Mean and raw values of T_1 and T_2 for each tissue are tabulated and/or plotted versus frequency and the fitting parameters A, B and the standard deviations determined to establish the normal range of relaxation times applicable to NMR imaging. The mechanisms for tissue NMR relaxation are reviewed with reference to the fast exchange two state (FETS) model of water in biological systems, and an overview of the dynamic state of water and macromolecular hydrogen compatible with the frequency, temperature, and multicomponent data is postulated. This suggests that ^{1}H tissue T_1 is determined predominantly by intermolecular (possibly rotational) interactions between macromolecules and a single bound hydration layer, and the T_2 is governed mainly by exchange diffusion of water between the bound layer and a free water phase. Deficiencies in measurement techniques are identified as major sources of data irreproducibility.

Key words: NMR relaxation, T_1, T_2, review, biological tissue, NMR imaging, relaxation mechanisms

I. INTRODUCTION

Longitudinal (T_1) and transverse (T_2) nuclear magnetic resonance (NMR) relaxation times play a pivotal role in the understanding of molecular level organization of biological systems in general and in NMR imaging in particular. Differences amongst hydrogen (^{1}H) NMR relaxation times of normal and pathological tissue are key to NMR image contrast and the discrimination of disease,[1–161] a fact responsible for their widespread use as diagnostic parameters in clinical NMR imaging. They directly effect the selection of imaging pulse sequence timing parameters,[51] and consequently, the total image scan times and patient throughput. They also influence the choice of the optimum magnetic field strength for NMR imaging because of their significant variation with NMR frequency.[22,55,73]

Since the early ^{1}H relaxation time studies on animal and human tissue by Odelblad *et al.* in the late 1950s,[89,120–124] the observation of elevated T_1's in cancer by Damadian in 1971,[40] and the more general T_1 variations in pathologies reported by Eggleston *et.al.* in 1975,[52] the literature has burgeoned with hundreds of investigations of relaxation time behavior in biological tissue. The majority of publications that report tissue relaxation time measurements ignore or make few attempts to interpret the physical mechanisms responsible for tissue relaxation or to compare them with similar published data, although the issues of species, frequency, temperature, and *in vivo/in vitro* dependence offer mitigating reasons. Moreover, efforts to collate this vast body of relaxation time information for the purpose of establishing the range of normal values and their frequency dependence are nonexistent.

This article reviews the published ^{1}H relaxation time data from normal human and animal tissues in an attempt to establish the normal range of T_1 and T_2 values for NMR imaging and their dependence on tissue type, NMR frequency, species, temperature, time after excision, *in vitro* versus *in vivo* measurement, and age. The data are presented graphically, to illustrate trends and deficiencies with the work to date; in tabular form, for locating sources, providing additional information, and for future collation; and as parameters of best fit to a simple expression, to enable rapid computation of the T_1 at any desired frequency. Since

 0094-2405/84/040425-24$01.20

whole-body ^{1}H NMR imaging systems currently operate within the frequency range of 1 to 65 MHz, with even higher frequencies imminent,[22,23] data extending over the frequency range 1–100 MHz are examined. Experimental results are analyzed theoretically in terms of available fast exchange two state (FETS) models involving water in essentially free and bound phases in biological tissues, thereby providing a cogent description of the spectrum of ^{1}H T_1 and T_2 relaxation mechanisms and molecular motions. A similar study of pathological tissue relaxation time data is underway.[24]

II. METHODS

A current awareness subscription from the New England Research Application Center was conducted from 1980 to 1983 to monitor the abstracting service data bases AGRICOLA (agricultural literature), Biological Abstracts, the Conference Papers Index, Energy Abstracts, the Engineering Index, Index Medicus, INSPEC (physics, electronics and computer abstracts), NTIS (government technical reports), SPIN (physics information), and the US Government Patent File. The search was keyed to tissue NMR relaxation time measurements, NMR imaging, and authors publishing in these research domains. Publications on tissue relaxation times prior to 1980 were searched by cross referencing personal files of papers collected since 1975, in addition to papers cited in the abstracting subscription. This procedure netted about 300 relevant articles by December 1983. One-half of these were rejected either because they contained no explicit relaxation time data for normal tissue; or because the NMR frequency (or field strength) was not stated; or because the relaxation times pertained only to isolated cell cultures, blood serum, plasma, dehydrated or homogenized tissues; or because measurements were performed below 0 °C; or because measurements were taken from tumor or pathology bearing animals; or because T_2 values were calculated from resonance linewidths. Of the remainder, results were presented in the text or in tables or in graphs. Where graphical information was the sole source, relaxation time information was read from the curves directly, thereby introducing some reading error. Arithmetic means are assumed for data tabulated as ranges. Data recorded *in vivo*, from fetal or immature tissue, or under other special circumstances are noted. Finally, data were checked for duplication in publications by the same authors, and in reviews.

III. RESULTS

A. Tissue, species, and frequency dependence

^{1}H NMR T_1 and T_2 data from normal liver, muscle (skeletal and heart), kidney, spleen, brain (grey and white matter), adipose, breast, lung, body fluids (blood, marrow, cerebral spinal fluid, amniotic fluid, bile, urine) and other miscellaneous tissues are presented in Tables 2–11, respectively. Table 1 summarizes the abbreviations used and the symbol legend for the plotted data. The mean cited standard deviation for each relaxation data point, expressed as a percentage of the T_1 and T_2 values, is about $(10 \pm 10)\%$ for all tissues. T_1 relaxation is typically characterized by a single-component exponential on a timescale > 5 ms except in several reports of *in vivo* and *in vitro* measurements of mouse liver and embalmed human liver and muscle,[5] *in vivo* newt tails,[141] *in vitro* rat muscle,[35] and *in vitro* human breast tissue[25,101,113] where dual, relatively long (> 50 ms) T_1 components of comparable magnitude were measured.

The T_1 frequency dispersions of tissues with sufficient data are plotted in Figs. 1–8. Where papers present data recorded at several temperatures, only those closest to physiological values are depicted. Fetal and immature tissue data are excluded from the plots because of their vastly elevated values. Different symbols denote human, rat, mouse, chicken, cow, pig, dog, gerbil, hamster, rabbit, frog, and newt contributions. Skeletal and heart muscle (Fig. 2), and grey and white brain matter (Fig. 5) have different T_1's and, therefore, are differentiated where possible. Similarly, kidney cortex and medulla have significantly different T_1's, but because few authors make such distinction, segregation of the kidney plot is impractical. Thus Fig. 3 should be regarded cautiously, as an organ average only. Note that for a given tissue type, there is no detectable difference in correlation between T_1 points and NMR frequency due to differences in species (Fig. 1–9), despite individual observations of T_1 differences amongst species by some researchers (Tables 2–11).

Curves of the form

$$T_1 = A\nu^B, \tag{1}$$

where A and B are constants and ν is the NMR frequency, are fitted to liver, muscle, kidney, spleen, brain, adipose, and lung T_1 dispersions combining all species, using the method of minimizing the sum of the squares of the fractional difference of T_1 data from the curve. Conventional fitting routines that minimize the sum of the squares of the absolute differences between the curve and the data preferentially weight the less numerous high-frequency points. This generates curves that appear better, but have slightly higher fractional errors. Power series expansions, and the dipolar expression for T_1 with a single correlation time (see Sec. IV A) diverge or are less successful at fitting data at extreme frequencies. However, the Escanye *et al.* relation[54]

$$T_1^{-1} = A'\nu^{-1/2} + B', \tag{2}$$

(A', B', constants) yields quite comparable results. A best fit to the Escanye *et al.* expression is plotted in Figs. 1 and 4 for comparison. Values of the fitting coefficients and the percentage standard deviations (assuming random distributions) of T_1 values from the curves for each tissue are tabulated in Table 12. The curves are not weighted with the number of samples averaged for each point because the scatter in T_1 values measured at the same frequency often greatly exceeds the cited standard deviations. The concentration of disagreeable data around 15 and 20 MHz attests to this. For breast tissue (Fig. 7), where the scatter exceeds 400%, curves from muscle and adipose plots [Figs. 2(a) and 6] are superimposed on the data suggesting tissue heterogeneity as the main cause: breast tissue is apparently a mixture of fibrous and fatty components. The applicability of the curve-fitting algorithm to individual T_1 dispersion data is demonstrated in Fig. 9 with measurements from Escanye *et al.*,[54] and Koenig *et al.*[99]

Tabulated tissue T_2 values appear essentially independent

Table 1.

KEY TO SYMBOLS USED IN THE TABLES 2-11 AND FIGURES 1-10.

A	= Auricle	P	= Pregnant
B	= Breast	Pa	= Parenchyma
C	= Cortex	R	= Red muscle
Cl	= Clotted	Ref	= Reference
de	= Day embryo	RT	= Room temperature
Di	= Dead intact	S	= Solid component
do	= Day old	Sh	= Short component
F	= Fetus	SL	= Semi liquid component
Freq	= Frequency	SS	= Semi solid component
Hp	= Heparinised	T	= Temperature at which measurements were made
I	= Immature	V	= Vivo
Intc	= Intercostal	Ven	= Ventricle
L	= Liquid component	Verte	= Vertebral
Lac	= Lactating	Vgn	= Virgin
Lo	= Long component	W	= White muscle
M	= Medium component	—	= Not reported
Med	= Medulla	%	= Percent of total proton population contribution to this component
N	= Number of samples		

Species:

⊙ — rat	| — newt (Figure 1) or cow (Figure 5)
× — chicken	+ — hamster
△ — dog	↑ — frog
⊡ — mouse	↓ — pig
★ — gerbil	▽ — rabbit
◇ — human	

Units:

T_1 and T_2 are in ms, frequencies are in MHz, and temperatures are in degrees °C.

Note:

In Table 8 the 17, 65 and 75 which precede Lo and Sh indicate the percentage of tissue fat in the breast sample.

of frequency. Figure 10 illustrates the T_2 dispersion for liver. T_2 data scatter is significantly greater than for T_1. Many researchers report multiple (≤ 4) T_2 components that constitute between 6% and 76% of the total observed tissue NMR signal intensity (Tables 2–11). Only the single T_2 component values are used in Fig. 10 and in computing the average T_2 values listed in Table 12.

B. Temperature dependence

The vast majority of tabulated relaxation data were measured either at room temperature (~23 °C) for *in vitro* studies, or physiological temperature (~37 °C) for *in vivo* measurements. The effect of temperature on T_1 was noted by Frey *et al.*[59] and Damadian *et al.*[42] The former reported that mice spleen T_1 depends "only mildly" on temperature from 5–40 °C, whereas the latter commented that "temperature control was found to be important" in the precise determination of T_1's. Neither group presented data supporting these assertions.

Quantitative investigations were undertaken by Barroilhet and Moran,[5] Escanye *et al.*,[54,55] Finch and Homer,[57] Fung,[62] Fung and McGaughy,[64] Fung *et al.*,[63] Parker *et al.*,[125] Koenig *et al.*,[99] and Lewa and Majewska.[102] Barroilhet and Moran concluded that "in general, relaxation times are strongly temperature dependent," although the principal effect of a temperature increase was an elevation in the longer of the dual T_1 components observed in embalmed human tissue, whereas the initial slope average T_1 in two samples increased less than 7% between 20 and 33 °C. Escanye *et al.* recorded mice T_1's of muscle, spleen, liver, and kidney at 20 (Ref. 54) and 24 °C[55] and at NMR frequencies between 10 and 90 MHz without significant difference. Over

Table 2. Liver

T1	T2	Freq	N	T	Species	Ref
100	-	1.0	1	35	dog	99
120	-	1.0	1	35	rabbit	99
84	-	1.0	1	-	rat	85
107	-	1.0	1	30	rat	99
123	-	1.6	1	30	rat	99
155	-	1.7	20	V	human	90,147,148,149,150
105	-	2.0	1	-	rat	85
133	-	2.0	1	30	rat	99
141	-	2.5	3	20	rabbit	105
138	36	2.7	10	19	mouse	38
133	-	3.0	1	35	dog	99
182	-	3.0	1	35	rabbit	99
154	-	3.0	1	30	rat	99
194	-	4.3	-	V	rabbit	70
215	37	4.3	-	V	rabbit	70,71
210	-	4.5	-	37	mouse	63
190	-	4.5	-	28	mouse	63
186	49	5.0	50	RT	rat	156
153	-	5.0	1	-	rat	85
200	-	5.0	1	30	rat	99
161	44	5.1	6	-	dog	160,161
160	-	5.1	6	25	rabbit	160
250	-	6.5	10	V	human	129
240	-	6.5	12	V	human	49,154
392	-	6.7	-	20	mouse	54
229	-	7.0	1	30	rat	99
250	-	7.5	-	37	mouse	63
215	-	7.5	-	28	mouse	63
240	-	8.0	1	20	mouse	5
228	-	8.0	10	V	mouse	5
251	-	8.0	11	-	mouse(Di)	5
165	-	8.0	2	-	rat	58
172	-	8.0	3	-	rat	58
163	-	8.0	2	-	rat	58
153	-	8.0	2	-	rat	58
380	40	8.5	10	V	human	139
171	-	10.0	1	35	dog	99
275	-	10.0	-	20	mouse	54
275	-	10.0	20	24	mouse	55
267	-	10.0	1	35	rabbit	99
205	-	10.0	1	-	rat	85
232	-	10.0	1	30	rat	99
225	-	10.7	2	RT	rat	33
235	-	10.7	4	-	rat	18
-	47	10.7	8	-	rat	18
300	-	12.0	-	37	mouse	63
275	-	12.0	-	28	mouse	63
238	-	13.6	4	-	rat	17
-	49	15.0	11	V	human	158
293	37	15.0	10	19	mouse	38
-	25	15.0	1	25	mouse	59
-	30	15.0	1	25	mouse	59
315	-	15.0	-	20	mouse	54
267	-	15.0	1	30	rat	99
418	37	15.0	16	V	rat	152
520	40	15.0	-	V	rat	43,44,80
420	38	15.0	8	V	rat	43,44,80
222	-	15.0	1	-	rat	85
396	-	17.1	-	25	mouse	108
285	-	17.1	-	25	rat	108
182	-	20.0	1	35	dog	99
397	96	20.0	3	40	human	72
350	-	20.0	-	20	mouse	54
375	-	20.0	20	24	mouse	55
411	-	20.0	20	RT	mouse	112
325	-	20.0	-	37	mouse	63
300	-	20.0	-	28	mouse	63
280	-	20.0	-	22	newt	141
182	41	20.0	8	40	pig	72
356	-	20.0	1	35	rabbit	99
281	32	20.0	16	-	rat	137
320	-	20.0	1	30	rat	99
250	40	20.0	54	23	rat	46
205	63	20.0	6	40	rat	72
271	38	22.5	5	-	rat	68
339	-	24.0	-	-	human	109
350	-	24.0	10	26	mouse	12,39
283	-	24.0	1	RT	mouse	84
296	-	24.0	1	RT	mouse	84
271	-	24.0	10	RT	mouse	84
263	-	24.0	1	RT	mouse	12,84
400	-	24.0	-	-	rabbit	109
311	-	24.0	3	23	rabbit	105
309	-	24.0	-	-	rabbit	109
324	-	24.0	-	-	rat	109
309	-	24.0	12	25	rat	50
296	-	24.0	72	-	rat	106
293	52	24.0	5	-	rat	12,40
301	-	24.3	1	26	dog	39
303	-	24.3	5	26	hamster	39
383	-	24.3	8	26	human	39
280	-	24.3	10	23	mouse	142
225	-	24.3	4	23	mouse	86
-	51	24.3	2	26	mouse	39
353	-	24.3	4	26	rabbit	39
205	-	24.3	32	23	rat	86
270	-	24.3	-	24	rat	87
721	-	25.0	1	23	human(F)	94
375	-	25.0	6	25	mouse	144
370	-	25.0	-	20	mouse	54
426	-	25.0	26	25	mouse	144
274	-	25.0	1	-	rat	85
438	-	25.3	27	-	mouse	134
273	-	25.3	3	RT	rat	12,37
-	53	25.6	5	33	hamster	103
-	48	25.6	5	33	hamster	103
-	68	25.6	5	33	hamster	103
298	-	30.0	4	-	human	92
385	-	30.0	-	20	mouse	54
341	-	30.0	25	-	mouse	92
400	-	30.0	20	24	mouse	55
386	-	30.0	7	25	mouse	59
361	-	30.0	2	-	mouse	92
382	-	30.0	1	25	mouse	59
356	-	30.0	1	30	rat	99
-	47	30.0	-	-	rat	34
412	33	30.3	6	25	mouse	12,76
438	33	30.3	6	25	mouse	12,76
208	-	32.0	6	25	chicken	12,136
475	-	35.0	-	37	mouse	63
425	-	35.0	-	28	mouse	63
410	-	36.5	-	20	mouse	54
-	78	60.0	1	22	human(Lo)	146
-	12	60.0	1	22	human(Sh)	146
520	-	60.0	20	24	mouse	55
531	-	60.0	11	27	mouse	4
630	-	60.0	-	37	mouse	63
560	-	60.0	-	28	mouse	63
467	-	60.0	4	25	rat	12,26
580	33	60.0	2	RT	rat	95
340	30	60.0	2	20	rat	96,97
527	43	60.0	2	20	rat(I)	96,97
640	-	90.0	20	24	mouse	55
635	-	90.0	-	20	mouse	54
570	-	100.0	14	26	human	12,41,42
420	37	100.0	-	-	mouse	12,91
550	30	100.0	5	-	mouse	91
637	-	100.0	4	-	rat	17
612	-	100.0	4	-	rat	18

Table 3. Muscle

T1	T2	Freq	N	T	Species	Ref
(a.) Skeletal Muscle						
230	56	1.0	-	25	frog	78
118	-	1.0	1	-	rat	85
151	-	1.1	-	25	mouse	62
130	-	1.7	-	V	human	150
180	-	1.7	-	V	human	90
130	-	1.7	-	V	human	148
184	-	1.7	1	V	rabbit	104
163	-	1.7	1	-	rabbit(Di)	104
150	-	2.0	1	-	rat	85
175	-	2.3	-	25	mouse	62
182	-	2.5	3	20	rabbit	105
183	-	2.5	3	20	rabbit(Abd)	105
191	-	2.5	3	20	rabbit(Intc)	105
181	42	2.5	36	20	rat	104
185	49	2.7	10	19	mouse	38
270	-	3.5	-	25	mouse	62
290	64	4.0	-	25	frog	78
312	-	4.0	-	25	mouse	62
250	40	4.3	-	-	frog	28
241	-	4.3	-	V	rabbit	70
264	-	4.3	-	V	rabbit	70
-	21	4.3	-	V	rabbit	70
259	28	4.3	-	V	rabbit	70,71
165	-	4.3	-	-	rabbit	70
225	-	4.3	-	-	rabbit(Di)	70
323	-	4.5	-	37	mouse	62
294	-	4.5	-	28	mouse	62
310	-	4.5	2	30	rat	64
-	65	5.0	-	25	frog	78
310	-	5.0	-	25	mouse	61
333	-	5.0	-	25	mouse	62
240	-	5.0	1	-	rat	85
270	64	5.1	5	25	dog	160,161
245	-	5.1	6	25	rabbit	160
333	-	6.0	-	25	mouse	62
360	-	6.7	-	20	mouse	54
420	63	7.0	-	25	frog	78
385	-	7.5	-	37	mouse	62
345	-	7.5	-	28	mouse	62
400	-	7.5	2	30	rat	64
345	-	8.0	-	25	mouse	62
480	64	8.5	-	25	frog	78
400	50	8.6	10	V	human	139
460	-	10.0	20	24	mouse	55
461	-	10.0	-	20	mouse	54
525	-	10.0	10	-	rat	130
301	-	10.0	1	-	rat	85
450	-	10.5	2	30	rat	64
376	-	10.7	2	RT	rat	33
404	-	13.6	4	-	rat	17
400	-	14.0	-	25	mouse	62
541	35	15.0	13	V	human	116
476	51	15.0	10	20	mouse	38
-	36	15.0	2	25	mouse	59
529	-	15.0	-	20	mouse	54
744	30	15.0	5	V	rat	115
356	33	15.0	3	V	rat	81
620	29	15.0	11	V	rat	81
596	33	15.0	11	V	rat	81
355	-	15.0	1	-	rat	85
725	32	15.0	21	V	rat	44
700	28	15.0	5	V	rat	45
510	-	16.5	2	30	rat	64
488	-	17.0	-	25	mouse	98
610	-	17.1	-	25	mouse	108
1246	-	20.0	5	36	chicken(1do)	114
746	-	20.0	5	36	chicken(8do)	114
647	-	20.0	5	36	chickn(16do)	114
1234	-	20.0	5	36	chickn(18de)	114
1244	-	20.0	5	36	chickn(20de)	114
390	47	20.0	-	14	frog	57
650	63	20.0	-	25	frog	78
629	45	20.0	3	40	human	72
528	-	20.0	20	RT	mouse	112
523	-	20.0	20	RT	mouse	112
500	-	20.0	-	25	mouse	62
599	-	20.0	-	20	mouse	54
600	-	20.0	20	24	mouse	55
556	-	20.0	-	37	mouse	62
488	-	20.0	-	28	mouse	62
605	58	20.0	8	40	pig	72
400	-	20.0	1	-	rat	85
576	61	20.0	6	40	rat	72
581	-	22.0	-	25	mouse	98
517	50	22.5	5	-	rat	68
536	51	22.5	5	-	rat	68
400	40	24.0	-	-	frog	28
575	-	24.0	5	-	human	109
415	-	24.0	1	RT	mouse	84
372	-	24.0	1	RT	mouse	84
411	-	24.0	10	RT	mouse	84
471	-	24.0	1	RT	mouse	12,84
554	-	24.0	3	23	rabbit	105
500	-	24.0	-	-	rabbit	109
534	-	24.0	3	23	rabbit(Abd)	105
600	-	24.0	-	-	rabbit(Abd)	109
519	-	24.0	3	23	rabbit(Intc)	105
600	-	24.0	-	-	rabbit(Intc)	109
538	55	24.0	5	-	rat	12,40
596	-	24.0	18	25	rat	107
807	-	24.3	2	26	human	39
475	-	24.3	4	23	mouse	142
465	-	24.3	4	23	mouse	86
525	-	24.3	-	24	rat	87
641	-	25.0	-	20	mouse	54
449	-	25.0	1	-	rat	85
-	195	25.0	-	24	rat(Lo,10%)	75
-	45	25.0	-	24	rat(M,82%)	75
-	5	25.0	-	24	rat(Sh,8%)	75
575	-	25.6	10	25	rat,cow	102
588	-	26.0	-	25	mouse	98
490	46	26.5	-	14	frog	57
700	44	27.5	-	23	frog	57
574	-	30.0	7	-	human	92
635	-	30.0	1	25	mouse	59
563	-	30.0	3	-	mouse	92
660	-	30.0	20	24	mouse	55
590	-	30.0	25	-	mouse	92
690	-	30.0	-	20	mouse	54
680	-	30.0	-	25	mouse	61
615	-	30.0	8	25	mouse	59
625	-	30.0	-	25	mouse	62
637	-	30.0	-	25	mouse	98
586	-	30.0	4	-	mouse(P)	92
608	-	30.0	-	25	rat	8
642	-	32.0	6	25	chicken(R)	136
598	-	32.0	6	25	chicken(W)	136
700	-	33.5	2	30	rat	64
800	60	33.8	-	21	mouse	140
-	143	33.8	-	20	mouse(L,7%)	128
-	2	33.8	-	20	mouse(S,11%)	128
-	41	33.8	-	20	mouse(SL,76%	128
-	503	33.8	-	20	mouse(SS,6%)	128
800	58	35.0	-	25	frog	78
684	-	35.0	-	25	mouse	98
667	-	35.0	-	37	mouse	62
589	-	35.0	-	28	mouse	62
730	-	36.5	-	20	mouse	54
741	-	41.0	-	25	mouse	98
725	-	43.5	5	37	human	21
762	-	45.0	-	25	mouse	98
-	168	60.0	30	20	frog(Lo,15%)	14
-	38	60.0	30	20	frog(M,67%)	14
-	10	60.0	30	20	frog(Sh,18%)	14
740	-	60.0	11	27	mouse	4
875	-	60.0	20	24	mouse	55
667	-	60.0	-	25	mouse	62
1111	-	60.0	-	37	mouse	62
769	-	60.0	-	28	mouse	62
1000	-	60.0	2	-	rat	64
850	-	60.0	6	25	rat	12,26
950	63	63.0	-	25	frog	78
1053	-	90.0	-	20	mouse	54
1050	-	90.0	20	24	mouse	55
1023	-	100.0	17	26	human	11,12,41,42
1100	-	100.0	-	25	mouse	61
950	45	100.0	5	-	mouse	91
850	57	100.0	5	20	mouse	12,91
1138	-	100.0	4	-	rat	17
(b.) Heart Muscle						
187	-	1.0	1	30	rat	99
250	-	1.7	-	V	human	90,148
295	-	2.5	3	20	rabbit(A)	105
243	-	2.5	3	20	rabbit(Ven)	105
333	70	5.1	6	25	dog	160,161
263	-	5.1	6	25	rabbit	160
434	-	10.7	2	RT	rat	33
650	42	15.0	6	-	dog	82
-	35	15.0	1	25	mouse	59
-	45	15.0	1	25	mouse	59
630	-	17.1	-	25	mouse	108
644	75	20.0	3	40	human	72
576	-	20.0	20	-	mouse	112
688	71	20.0	8	40	pig	72
654	70	20.0	6	40	rat	72
590	43	20.0	-	37	rat(Lo)	20
-	13	20.0	-	37	rat(Sh)	20
480	-	23.3	6	23	mouse	142
486	-	24.0	1	RT	mouse	84
490	-	24.0	1	RT	mouse	84
476	-	24.0	1	RT	mouse	84
706	-	24.0	3	23	rabbit(A)	105,109
637	-	24.0	3	23	rabbit(Ven)	105
700	-	24.0	-	-	rabbit(Ven)	109
481	-	24.0	-	25	rat	50
873	-	24.3	5	26	human	39
550	-	24.3	-	24	rat	87
518	-	25.3	3	RT	rat	37
620	-	25.6	10	25	rat,cow	102
664	-	30.0	1	25	mouse	59
650	-	30.0	7	25	mouse	59
936	69	60.0	2	20	mouse(I)	96,97
873	46	60.0	3	20	rat	96,97
906	-	100.0	9	26	human	41,42

Table 4. Kidney

T1	T2	Freq	N	T	Species	Ref
160	-	1.0	1	30	rat	99
320	-	1.7	20	V	human	90,147,148,150,151
200	-	2.0	1	30	rat	99
206	-	2.5	3	20	rabbit(C)	105
426	-	2.5	3	20	rabbit(Med)	105
214	56	2.7	10	19	mouse	38
229	-	3.0	1	30	rat	99
335	-	4.3	-	-	rabbit	70
-	70	4.3	-	V	rabbit	70,71
419	-	4.3	-	V	rabbit	70,71
359	-	4.3	-	V	rabbit	70
419	39	4.3	-	V	rabbit	70
230	-	4.3	-	V	rabbit(C)	70
433	-	4.3	-	-	rabbit(Di)	70
520	-	4.3	-	V	rabbit(Med)	70
320	-	5.0	1	30	rat	99
312	69	5.1	6	-	dog(C)	161
604	171	5.1	6	-	dog(Med)	161
216	-	5.1	6	25	rabbit(C)	160
473	-	5.1	6	25	rabbit(Med)	160
319	-	6.7	-	20	mouse	54
360	-	7.0	1	30	rat	99
670	50	8.5	10	V	human	139
370	-	10.0	-	20	mouse	54
260	-	10.0	20	24	mouse	55
400	-	10.0	1	30	rat	99
342	-	10.7	2	RT	rat	33
410	-	13.6	-	-	rat	17
670	57	15.0	-	V	human(C)	88
516	-	15.0	23	V	human(Pa)	53
-	35	15.0	1	25	mouse	59
415	-	15.0	-	20	mouse	54
390	59	15.0	10	19	mouse	38
-	42	15.0	1	25	mouse	59
467	-	15.0	1	30	rat	99
671	52	15.0	1	V	rat(Pa)	27
524	-	17.1	-	25	mouse	108
634	-	17.1	-	25	rat	108
765	124	20.0	3	40	human	72
450	-	20.0	20	24	mouse	55
391	-	20.0	20	RT	mouse	112
455	-	20.0	-	20	mouse	54
405	96	20.0	8	40	pig	72
533	-	20.0	1	30	rat	99
510	81	20.0	6	40	rat	72
459	-	24.0	-	25	human	12,84
370	-	24.0	1	RT	mouse	84
314	-	24.0	1	RT	mouse	84
290	-	24.0	-	25	mouse	50
286	-	24.0	1	RT	mouse	84
294	-	24.0	10	RT	mouse	84
500	-	24.0	-	-	rabbit	109
406	-	24.0	3	23	rabbit(C)	105
801	-	24.0	3	23	rabbit(Med)	105
480	-	24.0	5	-	rat	40
450	-	24.0	3	-	rat	106
534	-	24.3	1	26	dog	39
398	-	24.3	4	26	hamster	39
770	-	24.3	4	26	human	39
396	-	24.3	10	26	mouse	39
330	-	24.3	10	23	mouse	142
-	52	24.3	2	25	mouse	39
322	-	24.3	4	23	mouse	86
363	-	24.3	2	26	rabbit	39
390	-	24.3	-	24	rat	87
365	-	24.3	32	23	rat	86
993	-	25.0	1	23	human(F)	94
581	-	25.0	6	25	mouse	144
612	-	25.0	15	25	mouse	144
490	-	25.0	-	20	mouse	54
577	-	25.3	3	RT	rat	37
520	-	30.0	1	25	mouse	59
526	-	30.0	-	20	mouse	54
449	-	30.0	3	-	mouse	92
520	-	30.0	20	24	mouse	55
452	-	30.0	25	-	mouse	92
470	-	30.0	9	25	mouse	59
-	61	30.0	-	-	rat	34
503	47	30.3	6	25	mouse	12,13,76
551	50	30.3	6	25	mouse	12,76
403	-	32.0	6	25	chicken	136
602	45	33.8	-	21	mouse	140
565	-	36.5	-	20	mouse	54
800	-	45.0	1	30	rat	99
577	-	60.0	11	27	mouse	4
700	-	60.0	20	24	mouse	55
760	27	60.0	2	RT	rat	95
685	56	60.0	2	20	rat	96,97
668	-	60.0	12	25	rat	26
860	-	90.0	20	24	mouse	55
870	-	90.0	-	20	mouse	54
862	-	100.0	13	26	human	41,42
903	-	100.0	-	-	rat	17

a wider temperature range of 4 to 25 °C, Finch and Homer reported increases in frog muscle T_1 from 0.4 to 0.53 s measured at 23.3 MHz: the dependence was linear with reciprocal of absolute temperature ($1/T$). Fung and colleagues studied mouse muscle and liver T_1's from 0.01 to 100 MHz over a temperature range of about − 70 to 40 °C: increases in T_1 (linear in $1/T$) of approximately 20%, 30%, and 40% between 17 and 37 °C at 7.5, 35, and 60 MHz were measured, respectively. Parker *et al.* observed an essentially linear increase in blood T_1 between 0 and 50 °C with the increase between 20 and 37 °C being about 30% at 15 MHz. The T_1 values also varied linearly with $1/T$. Similarly, Koenig *et al.* measured T_1 increases of 23% at 1 MHz to 85% at 20 MHz as a result of increasing the temperature of rabbit blood from 5 to 35 °C. Lewa and Majewska presented a comprehensive study of rat and cow liver, muscle, heart, spleen, and lung tissue T_1's over a 10 to 70 °C temperature range at 15.6 MHz. Their data (Fig. 11) indicate T_1 increases of about 10% between room and physiological temperatures, also linear in $1/T$.

Few investigations of the temperature dependence of tissue T_2's above freezing point were found. Finch and Homer[57] reported no change in frog muscle T_2 between 4 and 25 °C at 23.3 MHz, within experimental error. Belton *et al.*[14] reported a decrease in frog muscle T_2's with increasing temperature from 0 to 25 °C. The widespread observation of multiple T_2 components and large T_2 scatter (Fig. 10) renders dubious the value of analyzing the tabulated T_2 data for temperature dependence.

C. Time after excision

Tabulated *in vitro* data were recorded up to 12 h following excision or death. Therefore the dependence of tissue relaxation on time after excision is another potential source of variation amongst *in vitro* data. It has been extensively studied.[5,8,35,37,39–42,45,59,68,84,99,126,127,141,156]

Frey *et al.*[59] and Hollis *et al.*[84] noted no appreciable change in mouse and human tissue T_1's kept at room temperature in air-tight tubes 12 to 24 h after excision. Damadian[40] measured decreases in T_1 of less than 10% from human liver, kidney, and brain. Cottam *et al.*[39] also measured T_1 changes of less than 10% in mouse liver, spleen, kidney, lymph node, and lymph sarcoma tissues kept at room temperature for 24 h. Damadian measured more marked decreases of 36% and 11% for human stomach and small intestine. Pearson *et al.*[127] observed no significant change in porcine muscle T_1 and in the dominant (short) T_2 component at 1.75 and 24 h postmortem. Similarly, Thickman *et al.*[156] reported constant T_1's of untreated rat liver and spleen tissue kept at room temperature for 6 h after excision, and declines in T_1 of only 12% and 18% in liver and spleen, respectively, after 24 h. They observed essentially no change in the T_2 of both rat liver and spleen samples over 48 h following excision. In apparent contrast, Small *et al.*[145] reported dual component T_2 measurements of human breast tissue which "decline significantly as a function of time" when stored at room temperature. Examination of the data, however, indicates

Table 5. Spleen

T1	T2	Freq	N	T	Species	Ref
240	-	1.0	1	35	rabbit	99
219	-	1.0	1	30	rat	99
150	-	1.0	1	-	rat	85
240	-	1.5	1	30	rat	99
270	-	1.7	20	V	human	90,148,149,150
125	-	2.0	-	-	mouse	48
246	-	2.0	1	30	rat	99
192	-	2.0	1	-	rat	85
258	-	2.5	3	20	rabbit	105
263	66	2.7	10	19	mouse	38
320	-	3.0	1	35	rabbit	99
291	-	3.0	1	30	rat	99
261	63	5.0	50	RT	rat	156
400	-	5.0	1	30	rat	99
344	107	5.1	6	30	dog	161
333	-	5.1	6	25	rabbit	160
510	-	6.5	-	V	human	49,129,154
405	-	6.7	-	20	mouse	54
457	-	7.0	1	30	rat	99
287	-	8.0	2	-	rat	58
273	-	8.0	4	-	rat	58
278	-	8.0	2	-	rat	58
420	20	8.5	-	V	human	139
480	-	10.0	20	24	mouse	55
481	-	10.0	-	20	mouse	54
533	-	10.0	1	35	rabbit	99
533	-	10.0	1	30	rat	99
306	-	10.0	1	-	rat	85
443	-	10.7	2	RT	rat	33
-	61	15.0	11	V	human	158
-	45	15.0	1	25	mouse	59
-	35	15.0	1	25	mouse	59
493	70	15.0	10	19	mouse	38
549	-	15.0	-	20	mouse	54
426	-	17.0	-	25	mouse	98
641	-	17.1	-	25	mouse	108
461	-	17.1	-	25	rat	108
760	140	20.0	3	40	human	72
566	-	20.0	101	RT	mouse	112
606	-	20.0	-	20	mouse	54
600	-	20.0	20	24	mouse	55
507	64	20.0	8	40	pig	72
800	-	20.0	1	35	rabbit	99
385	-	20.0	1	-	rat	85
800	-	20.0	1	30	rat	99
431	94	20.0	6	40	rat	72
500	-	22.0	-	25	mouse	98
535	-	24.0	-	-	human	109
433	-	24.0	1	RT	mouse	84
399	-	24.0	1	RT	mouse	84
366	-	24.0	9	RT	mouse	84
458	-	24.0	1	RT	mouse	84
529	-	24.0	-	-	rabbit	109
509	-	24.0	3	23	rabbit	105,109
505	-	24.0	72	-	rat	106
531	-	24.0	-	-	rat	109
539	-	24.3	1	26	dog	39
600	-	24.3	1	26	hamster	39
567	-	24.3	1	23	human	67
519	-	24.3	1	23	human	67
680	-	24.3	10	26	human	39
425	-	24.3	5	23	mouse	142
-	61	24.3	2	26	mouse	39
571	-	24.3	9	26	mouse	39
614	-	24.3	3	26	rabbit	39
510	-	24.3	-	24	rat	87
658	-	25.0	20	25	human	144
712	-	25.0	14	25	mouse	144
637	-	25.0	-	20	mouse	54
406	-	25.0	1	-	rat	85
457	-	25.3	3	RT	rat	37
-	72	25.6	5	33	hamster	103
-	78	25.6	5	33	hamster	103
-	69	25.6	5	33	hamster	103
580	-	25.6	10	25	rat,cow	102
521	-	26.0	-	25	mouse	98
500	-	30.0	-	-	mouse	48
523	-	30.0	21	-	mouse	92
571	45	30.0	9	25	mouse	59
563	35	30.0	1	25	mouse	59
541	-	30.0	-	25	mouse	98
676	-	30.0	-	20	mouse	54
680	-	30.0	20	24	mouse	55
582	-	30.0	12	25	rat	26
671	45	30.3	6	25	mouse	76
737	55	30.3	6	25	mouse	76
596	-	32.0	6	25	chicken	12,136
-	33	33.7	10	23	mouse	47
700	40	33.8	-	21	mouse	140
578	-	35.0	-	25	mouse	98
752	-	36.5	-	20	mouse	54
625	-	41.0	-	25	mouse	98
645	-	45.0	-	25	mouse	98
800	-	45.0	1	30	rat	99
762	-	60.0	6	27	mouse	4
840	-	60.0	20	24	mouse	55
980	-	90.0	-	20	mouse	54
950	-	90.0	20	24	mouse	55
701	-	100.0	17	26	human	11,12,41,42

Table 6. Brain

T1	T2	Freq	N	T	Species	Tissue	Ref
255	-	1.7	-	V	human	cerebellum	147
275	-	1.7	-	V	human	grey-cerebrum	147
303	-	1.7	22	V	human	grey-frontal	16
299	-	1.7	22	V	human	grey-occipital	16
304	-	1.7	22	V	human	grey-parietal	16
287	-	1.7	-	V	human	grey.matter	148
262	-	1.7	-	V	human	grey.matter	90
255	-	1.7	-	V	human	spinal.cord	147
255	-	1.7	-	V	human	spinal.cord	90
225	-	1.7	-	V	human	white-cerebrum	147
244	-	1.7	22	V	human	white-frontal	16
250	-	1.7	22	V	human	white-occipital	16
248	-	1.7	22	V	human	white-parietal	16
232	-	1.7	-	V	human	white.matter	90
237	-	1.7	-	V	human	white.matter	148
410	-	1.7	-	V	human(I)	grey.matter	148
410	-	1.7	-	V	human(I)	white.matter	148
273	-	1.8	27	V	human	cerebel.cortex	65
248	-	1.8	27	V	human	cerebel.medul	65
288	-	1.8	27	V	human	grey-frontal	65
250	-	1.8	27	V	human	pontine.region	65
227	-	1.8	27	V	human	white-frontal	65
326	-	2.5	3	23	rabbit	cerebellum	105
308	-	2.5	3	23	rabbit	med.oblongata	105
325	-	2.5	3	23	rabbit	spinal.cord	105
285	75	2.7	9	19	mouse	-	38
410	-	5.0	3	25	mouse	homogenized	61
290	100	5.1	2	-	dog	brain.stem	161
429	115	5.1	3	-	dog	cerebellum	161
427	118	5.1	13	-	dog	grey.matter	161
345	114	5.1	3	-	dog	pituitary	161
350	98	5.1	2	-	dog	thalamus	161
262	133	5.1	11	-	dog	white.matter	161
399	-	6.3	1	V	human	-	29
515	-	6.5	10	V	human	grey-caudate.nuc	32
525	-	6.5	10	V	human	grey-crbrl.cortx	32
540	-	6.5	10	V	human	grey-inslr.cortx	32
430	-	6.5	10	V	human	grey-lentc.nuc.	32
375	-	6.5	10	V	human	grey-thalamus	32
-	110	6.5	6	V	human	grey.matter	3
295	-	6.5	10	V	human	white-frcps.mjr	32
285	-	6.5	10	V	human	white-frcps.mnr	32
-	105	6.5	6	V	human	white.matter	3
311	80	10.7	-	-	bovine	white.matter	66
405	-	10.7	2	RT	rat	-	33
585	90	12.8	4	V	human	cerebellum	157
710	100	12.8	4	V	human	cerebrum	157
600	115	12.8	4	V	human	cerebrum	157
490	90	12.8	4	V	human	cerebrum	157
600	100	12.8	4	V	human	cerebrum(ave)	157
380	80	12.8	4	V	human	corpus.callosum	157
600	100	12.8	2	V	human	grey.matter	157
475	100	12.8	4	V	human	medulla	157
445	75	12.8	4	V	human	pons	157
380	80	12.8	2	V	human	white.matter	157
474	-	13.7	4	-	rat	-	17
847	56	15.0	5	V	gerbil	cerebrum-l.hem	110
809	54	15.0	5	V	gerbil	cerebrum-r.hem	110
-	45	15.0	6	25	mouse	-	59
488	78	15.0	9	19	mouse	-	38
880	57	15.0	6	V	rat	-	44
640	-	17.1	-	25	rat	-	108
630	98	20.0	3	40	human	-	72
825	110	20.0	4	37	human	grey.matter	119
687	107	20.0	4	37	human	white.matter	119
584	-	20.0	20	RT	mouse	homoginized	112
713	102	20.0	8	40	pig	-	72
816	122	20.0	8	40	pig	cerebel.cortex	72
850	104	20.0	8	40	pig	grey-cerebrum	72
516	112	20.0	8	40	pig	pons	72
484	92	20.0	8	40	pig	spinal.cord	72
676	87	20.0	8	40	pig	white-cerebrum	72
589	70	20.0	6	40	rat	-	72
483	-	24.0	10	RT	mouse	-	84
517	-	24.0	3	RT	mouse	-	84
570	-	24.0	3	23	rabbit	cerebellum	105
700	-	24.0	-	-	rabbit	cerebellum	109
644	-	24.0	3	23	rabbit	grey.matter	105
700	-	24.0	-	-	rabbit	grey.matter	109
493	-	24.0	3	23	rabbit	med.oblongata	105,109
464	-	24.0	3	23	rabbit	spinal.cord	105
469	-	24.0	3	23	rabbit	white.matter	105
595	-	24.0	5	-	rat	-	40
590	-	24.3	-	24	mouse	-	87
795	-	24.3	5	23	mouse	cerebrum	142
472	-	25.3	3	RT	rat	-	37
693	-	30.0	1	25	mouse	-	59
646	-	30.0	6	25	mouse	-	59
800	-	30.0	3	25	mouse	homogenized	61
660	-	32.0	10	RT	rat	grey.matter	93
560	-	32.0	10	RT	rat	white.matter	93
-	88	60.0	15	32	dog	grey.matter	126
435	105	60.0	10	32	human	grey.matter	126
-	65	60.0	7	32	human	white.matter	126
1361	149	60.0	2	20	mouse(I)	-	96,97
866	71	60.0	3	20	rat	-	96,97
998	-	100.0	8	26	human	-	41,42
880	-	100.0	-	-	mouse	-	91
840	88	100.0	5	20	mouse	-	12,91,96
1030	-	100.0	3	25	mouse	homogenized	61
1174	-	100.0	4	-	rat	-	17
1146	76	100.0	5	25	rat	grey.matter	118
1078	76	100.0	5	25	rat	white.matter	118
1280	57	150.0	18	-	gerbil	-	30,31
1830	-	150.0	6	-	gerbil(1do)	-	30
1330	-	150.0	2	-	gerbil(21do)	-	30
1260	-	150.0	6	-	gerbil(21do)	-	30
1820	-	150.0	5	-	gerbil(2do)	-	30
1780	-	150.0	4	-	gerbil(8do)	-	30

Table 7. Adipose

T1	T2	Freq	N	T	Species	Ref
171	-	1.5	1	30	rat	99
130	-	1.7	-	V	human	90
145	-	1.7	28	V	human	148
70	-	1.7	40	V	human	150
146	-	1.8	3	V	human(B)	138
175	-	2.0	1	30	rat	99
187	-	3.0	1	30	rat	99
75	-	4.3	-	-	rabbit	70
183	-	4.3	-	V	rabbit	70,71
196	-	4.3	-	V	rabbit	70
-	63	4.3	-	V	rabbit	70
-	69	4.3	-	V	rabbit	70,71
172	-	4.3	-	V	rabbit	70
105	-	4.3	-	-	rabbit(Di)	70
75	73	5.1	5	-	dog	161
206	-	7.0	1	30	rat	99
240	60	8.5	10	V	human	139
213	-	10.0	1	30	rat	99
158	122	10.7	-	-	human	66
218	61	15.0	12	V	human	116
-	51	15.0	-	V	human	83
229	-	15.0	1	30	rat	99
305	57	15.0	5	V	rat	115
310	50	15.0	10	V	rat	43,44,45,80
192	108	20.0	3	40	human	72
192	105	20.0	8	40	pig	72
240	-	20.0	1	30	rat	99
221	173	20.0	6	40	rat	72
-	105	22.5	32	-	human	67
133	-	22.5	36	-	human	67
148	-	24.3	4	23	human	52
191	-	24.3	2	23	human(B)	52
190	-	24.3	-	24	rat	87
144	-	30.0	8	-	human	92
320	-	30.0	1	30	rat	99
320	-	45.0	1	30	rat	99
-	165	60.0	2	22	hum(BLo,61%)	145
-	52	60.0	2	22	hum(BSh,38%)	145
200	-	60.0	-	24	human(B)	25
245	-	60.0	3	27	mouse	4
279	-	100.0	5	26	human	41,42

Table 8. Breast

T1	T2	Freq	N	T	Species	Ref
126	-	1.8	22	-	human	138
337	-	13.6	4	-	rat(Lac)	17
447	46	22.5	12	-	human	67
554	46	22.5	11	-	human	67
510	-	24.0	6	-	human	109
191	-	24.3	2	23	human(Fat)	52
501	-	30.0	-	25	human	8
373	47	30.0	-	25	mouse(P)	6,9
682	36	30.3	7	25	human	12,113
380	39	30.3	5	25	mouse(P)	10,12,73
357	47	30.3	8	25	mouse(P)	12,76
275	84	30.3	22	25	mouse(Vgn)	9,11,12
-	155	60.0	-	22	hum(17Lo,62%)	145
-	52	60.0	-	22	hum(17Sh,38%)	145
-	182	60.0	-	22	hum(65Lo,59%)	145
-	57	60.0	-	22	hum(65Sh,41%)	145
-	157	60.0	-	22	hum(75Lo,60%)	145
-	50	60.0	-	22	hum(75Sh,40%)	145
907	-	60.0	15	24	human	25
200	-	60.0	15	24	human(Fat)	25
-	105	60.0	26	22	human(Lo)	146
-	23	60.0	26	22	human(Sh)	146
367	-	100.0	5	26	human	41
978	-	100.0	1	26	human(Lac)	41
980	-	100.0	4	-	rat(Lac)	17

Table 9. Lung

T1	T2	Freq	N	T	Species	Ref
293	-	2.5	6	20	rabbit	105
268	-	4.3	-	V	rabbit	70
423	-	4.3	-	V	rabbit	70
-	33	4.3	-	V	rabbit	70
374	98	5.1	6	-	dog	161
576	-	10.7	2	RT	rat	33
-	47	15.0	1	25	mouse	59
-	50	15.0	1	25	mouse	59
756	139	20.0	3	40	human	72
844	87	20.0	8	40	pig	72
586	78	20.0	6	40	rat	72
534	92	22.5	22	-	human	101
535	87	22.5	17	-	human	69
544	91	22.5	11	-	rat	68
403	-	24.0	2	RT	human	84
491	-	24.0	3	RT	mouse	84
700	-	24.0	-	-	rabbit	109
800	-	24.0	-	-	rabbit	109
655	-	24.0	6	23	rabbit	105
587	-	25.3	3	RT	rat	37
-	71	25.6	5	33	hamster	103
690	-	25.6	10	25	rat,cow	102
657	-	30.0	1	25	mouse	59
641	-	30.0	6	25	mouse	59
670	-	32.0	6	25	chicken	136
788	-	100.0	5	26	human	41,42

only a change of approximately 10% in long and short breast tissue T_2 components over a 24 h period.

Authors reporting dual T_1 components note contrary behavior of both components with time after excision. Chang *et al.*[35] measured an increase in the long rat muscle T_1 component to a maximum of about 16% at 3 h after excision. This was followed by a reduction to a level 5% above the initial value at 4 h after excision, where it remained constant for 27 h. The short T_1 component remained constant within 2% for the entire duration of the experiment. Sandhu and Friedmann[141] observed similar results, albeit on newt tails, except the long component increased 36% after 3 h and the short component declined 5% over 5 h postmortem. The opposite behavior in T_1 components of mouse liver measured *in vivo*, at 2.5 and at 3.5 h postmortem is indicated by Barroilhet and Moran.[5] Their results showed that the long T_1 component declined up to about 25%, whereas the short component first decreased about 10% then increased more than 10% after death. Their *in vivo* data for both components, however, show a 60% spread attributed to "intrinsic changes taking place in the tissue" which could easily explain their postmortem results. Moreover, while the behavior of multiple T_1 components with time after excision may not be clear, both Chang *et al.* and Barroilhet and Moran data demonstrate that variations in the combined, average effective T_1's are less than 10% during the periods studied.

A second class of experiments examined the effect of refrigeration of excised tissue samples prior to NMR measurements. Frey *et al.*,[59] Damadian *et al.*,[42] Parish *et al.*,[126] and Koenig *et al.*[99] all reported negligible or less than 10% variations in T_1 relaxation times of animal and human tissues stored at 4–5 °C for periods of up to a week after excision. In addition, Parish *et al.*[126] and Goldsmith *et al.*[68] compared surgical and autopsy samples. In the former study, excised dog grey matter brain specimens placed on ice (surgical

Table 10. Fluids

T1	T2	Freq	N	T	Species	Fluid	Ref
3300	-	1.0	-	37	human	amniotic.fluid	15
3400	-	3.0	-	37	human	amniotic.fluid	15
3600	-	7.0	-	37	human	amniotic.fluid	15
-	2300	100.0	-	37	human	amniotic.fluid	15
275	-	1.7	-	V	human	bile	147
380	-	1.7	-	V	human	bile	148
888	-	2.5	3	20	rabbit	bile	105
383	339	5.1	3	-	dog	bile	161
890	80	8.5	6	V	human	bile	139
805	-	15.0	3	-	dog	bile	117
1078	-	24.0	3	23	rabbit	bile	105
303	-	1.0	1	35	rabbit	blood	99
385	-	1.6	1	35	rabbit	blood	99
355	-	1.7	20	V	human	blood	147,148,149,150
444	-	2.0	1	35	rabbit	blood	99
404	-	2.5	3	20	rabbit(Cl)	blood	105
372	-	2.5	3	20	rabbit(Hp)	blood	105
500	-	3.0	1	35	rabbit	blood	99
667	-	5.0	1	35	rabbit	blood	99
571	261	5.1	6	-	dog	blood	161
833	-	7.5	1	35	rabbit	blood	99
909	-	10.0	1	35	rabbit	blood	99
472	-	10.7	2	RT	rat	blood	33
1000	-	15.0	1	35	rabbit	blood	99
900	-	19.8	20	33	human	blood	100
893	362	20.0	3	40	human	blood	72
902	-	20.0	20	RT	mouse	blood	112
800	-	20.0	-	22	newt	blood	141
1111	-	20.0	1	35	rabbit	blood	99
901	251	20.0	6	40	rat	blood	72
800	-	24.0	-	-	rabbit	blood	109
867	-	24.0	3	23	rabbit(Cl)	blood	105
872	-	24.0	3	23	rabbit(Hp)	blood	105
920	-	32.0	6	25	chicken	blood	136
900	-	1.7	-	V	human	cerebrospinal.fl	148
675	-	1.7	-	V	human	cerebrospinal.fl	147
-	915	6.5	6	V	human	cerebrospinal.fl	3
1450	-	6.5	10	V	human	cerebrospinal.fl	32
1155	145	12.8	1	V	human	cerebrospinal.fl	157
175	-	2.5	3	20	rabbit	marrow	105
306	-	4.3	1	V	rabbit	marrow	70,71
-	59	4.3	-	V	rabbit	marrow	70
-	17	4.3	-	V	rabbit	marrow	70
359	-	4.3	1	V	rabbit	marrow	70
271	-	4.3	1	V	rabbit	marrow	70
280	80	8.5	10	V	human	marrow	139
380	70	8.5	10	V	human(Verte)	marrow	139
320	80	12.8	4	V	human	marrow	157
420	50	15.0	16	V	human(Verte)	marrow	116
130	-	24.0	-	-	human	marrow	109
200	-	24.0	-	-	rabbit	marrow	109
202	-	24.0	3	23	rabbit	marrow	105
803	-	25.0	5	-	human	marrow	132
408	-	32.0	6	25	chicken	marrow	136
1000	-	1.7	-	V	human	urine	148
800	-	1.7	-	V	human	urine	147
2650	2600	5.1	3	-	dog	urine	161
2200	570	8.5	6	V	human	urine	139
3740	159	15.0	5	V	rat	urine	115

Table II. Miscellaneous

T1	T2	Freq	N	T	Species	Tissue	Ref
277	-	2.5	3	20	rabbit	adrenal	105
253	79	5.1	5	-	dog	adrenal	161
448	-	24.0	3	23	rabbit	adrenal	105,109
585	-	24.3	1	26	human	adrenal	39
608	-	100.0	5	26	human	adrenal	41,42
860	90	8.5	10	V	human	aorta	139
211	-	2.5	3	20	rabbit	aortic.arch	105
451	-	24.0	3	23	rabbit	aortic.arch	105,109
212	47	5.1	4	-	dog	artery	161
600	-	24.0	-	-	rabbit	bladder	109
891	-	100.0	3	26	human	bladder	41,42
200	-	1.7	-	V	human	bone	90
125	-	24.0	1	-	human	bone	109
200	-	24.0	-	-	rabbit	bone	109
554	-	100.0	10	26	human	bone	41,42
167	-	2.5	3	20	rabbit	carotid.artery	105
364	-	24.0	3	23	rabbit	carotid.artery	105
500	-	24.0	-	-	rabbit	carotid.wall	109
827	-	100.0	4	26	human	cervix	41,42
227	-	2.5	3	20	rabbit	colon	105
366	64	22.5	16	-	human	colon	101
388	56	22.5	12	-	rat	colon	68
475	-	24.0	1	RT	human	colon	84
300	-	24.0	-	-	rabbit	colon	109
466	-	24.0	3	23	rabbit	colon	105
552	-	24.3	2	23	human	colon	52
398	-	25.3	3	RT	rat	colon	37
641	-	100.0	12	26	human	colon	41,42
202	-	2.5	3	20	rabbit	diaphram	105
458	-	24.0	3	23	rabbit	diaphram	105
700	-	24.0	-	-	rabbit	diaphram	109
936	-	100.0	1	26	human	diaphram	41,42
309	-	2.5	2	20	rabbit	epididymus	105
625	-	24.0	2	23	rabbit	epididymus	105,109
250	-	2.5	3	20	rabbit	esophagus	105
534	-	24.0	3	23	rabbit	esophagus	105
804	-	100.0	5	26	human	esophagus	41,42
329	-	60.0	8	27	mouse	eyelens	4
1247	-	100.0	1	26	human	fallopian.tube	41,42
269	55	15.0	-	V	human	femoral.heads	79
416	58	22.5	28	-	human	gastrointestinal	68
201	-	2.5	3	20	rabbit	infer.venacava	105
316	-	24.0	3	23	rabbit	infer.venacava	105
2623	48	15.0	4	V	human	interverteb.disk	116
-	36	15.0	2	25	mouse	intestine	59
366	-	30.0	7	25	mouse	intestine	59
361	-	30.0	1	25	mouse	intestine	59
864	107	15.0	3	V	human	ligament/tendon	116
725	91	20.0	3	40	human	lymph.node	72
720	-	100.0	6	26	human	lymph.node	41,42
1050	75	100.0	5	-	mouse	lymph.node	91
200	-	24.0	-	-	rabbit	mesentery	109
111	58	5.1	3	-	dog	nerve	161
300	-	24.0	-	-	rabbit	nerve	109
557	-	100.0	2	26	human	nerve	41,42
310	-	2.5	1	20	rabbit	ovary	105
380	126	5.1	2	-	dog	ovary	161
600	-	24.0	3	-	human	ovary	109
573	-	24.0	1	23	rabbit	ovary	105
989	-	100.0	5	26	human	ovary	41,42
190	-	1.7	40	V	human	pancreas	147,148,150
231	43	5.1	3	-	dog	pancreas	161
290	60	8.5	-	V	human	pancreas	139
218	-	10.7	2	RT	rat	pancreas	33
572	189	20.0	3	40	human	pancreas	72
300	-	24.0	-	-	rabbit	pancreas	109
320	-	24.3	3	26	human	pancreas	39
605	-	100.0	10	26	human	pancreas	41,42
234	-	2.5	3	20	rabbit	parotid.gland	105
350	30	8.5	-	V	human	parotid.gland	139
340	-	24.0	3	23	rabbit	parotid.gland	105
476	-	100.0	1	26	human	peritoneum	41,42
1291	-	100.0	1	26	human	pineal.gland	41,42
1000	-	24.3	1	26	human	placenta	39
200	-	1.7	-	V	human	prostate	90
288	-	1.7	-	V	human	prostate	147
808	98	20.0	3	40	human	prostate	72
767	-	24.3	1	26	human	prostate	39
803	-	100.0	2	26	human	prostate	41,42
600	-	24.0	-	-	rabbit	rectum	109
245	-	2.5	3	20	rabbit	rectum.wall	105
492	-	24.3	3	23	rabbit	rectum.wall	105
400	-	24.0	-	-	rabbit	salivary.gland	109
384	-	60.0	8	27	mouse	salivary.gland	4
235	60	12.8	4	V	human	scalp	157
198	-	2.5	3	20	rabbit	skin	105
-	35	15.0	2	25	mouse	skin	59
450	-	24.0	6	-	human	skin	109
193	-	24.0	3	RT	mouse	skin	84
328	-	24.0	3	23	rabbit	skin	105
423	-	24.3	2	23	human	skin	52
225	-	24.3	5	23	mouse	skin	142
272	-	25.3	3	RT	rat	skin	37
-	65	25.6	5	33	hamster	skin	103
390	-	30.0	5	25	mouse	skin	59
722	-	30.0	1	25	mouse	skin	59
616	-	100.0	8	26	human	skin	41
224	-	2.5	3	20	rabbit	small.intestine	105
306	-	24.0	2	RT	mouse	small.intestine	84
400	-	24.0	-	-	rabbit	small.intestine	109
481	-	24.0	3	23	rabbit	small.intestine	105
257	-	24.0	5	-	rat	small.intestine	40
584	-	24.3	2	23	human	small.intestine	52
641	-	100.0	8	26	human	small.intestine	41,42
325	-	2.5	3	20	rabbit	spinal.cord	105
464	-	24.0	3	23	rabbit	spinal.cord	105
227	-	2.5	3	20	rabbit	stomach	105
-	35	15.0	2	25	mouse	stomach	59
400	-	24.0	-	-	rabbit	stomach	109
468	-	24.0	3	23	rabbit	stomach	105
270	-	24.0	5	-	rat	stomach	40
541	-	24.3	1	26	human	stomach	39
372	-	25.3	3	RT	rat	stomach	37
294	-	30.0	6	25	mouse	stomach	59
318	-	30.0	1	25	mouse	stomach	59
765	-	100.0	8	26	human	stomach	41,42
463	-	2.5	2	20	rabbit	testis	105
410	111	5.1	2	-	dog	testis	161
674	-	10.7	2	RT	rat	testis	33
974	153	20.0	3	40	human	testis	72
205	-	24.0	1	RT	mouse	testis	84
855	-	24.0	2	23	rabbit	testis	105
800	-	24.0	-	-	rabbit	testis	109
705	-	24.3	4	23	human	testis	52
1010	-	24.3	1	26	human	testis	39
1200	-	100.0	4	26	human	testis	41,42
809	-	24.3	1	26	human	thymus	39
605	102	20.0	3	40	human	thyroid	72
500	-	24.0	-	-	rabbit	thyroid	109
586	-	24.3	1	26	human	thyroid	39
409	-	24.3	2	23	human	thyroid	52
882	-	100.0	7	26	human	thyroid	41,42
584	61	20.0	3	40	human	tongue	72
560	58	20.0	8	40	pig	tongue	72
199	-	2.5	3	20	rabbit	trachea	105
276	-	24.0	3	23	rabbit	trachea	105,109
693	-	100.0	1	26	human	trachea	41,42
172	-	2.5	3	20	rabbit	ureter	105
252	-	24.0	3	23	rabbit	ureter	105,109
924	-	100.0	4	26	human	uterus	41,42
296	-	2.5	1	20	rabbit	uterus.wall	105
653	-	24.0	1	23	rabbit	uterus.wall	105
1019	-	100.0	2	26	human	vagina	41,42
550	-	24.0	2	-	human	vein	109

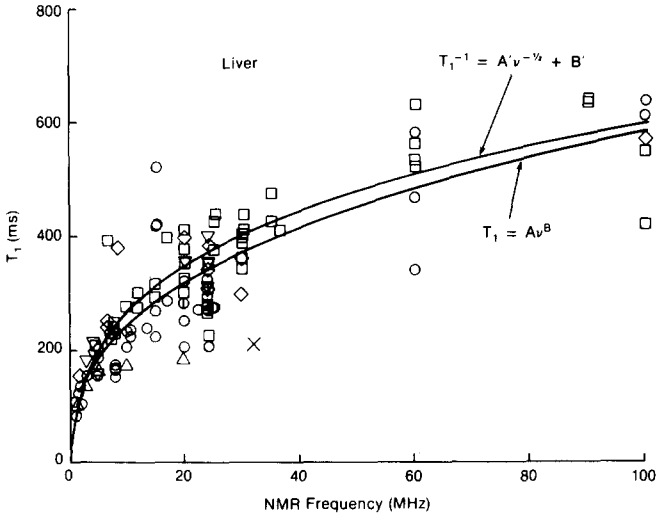

FIG. 1. T_1 dispersion data for liver fitted to $T_1 = A\nu^B$ with $A = 0.000\,534$, $B = 0.3799$ and standard deviation from the curve of 22% using a method of least squares. A least-squares fit to the Escanye *et al.* expression

$$T_1^{-1} = A'\nu^{-1/2} + B'$$

gave the same standard derivation and a best fit with $A' = 9807$, $B' = 0.689$. These parameters are the same as determined previously with less data (Ref. 54). The mean cited standard deviation for each point expressed as a percentage of the T_1 value is about $(9 \pm 5)\%$.

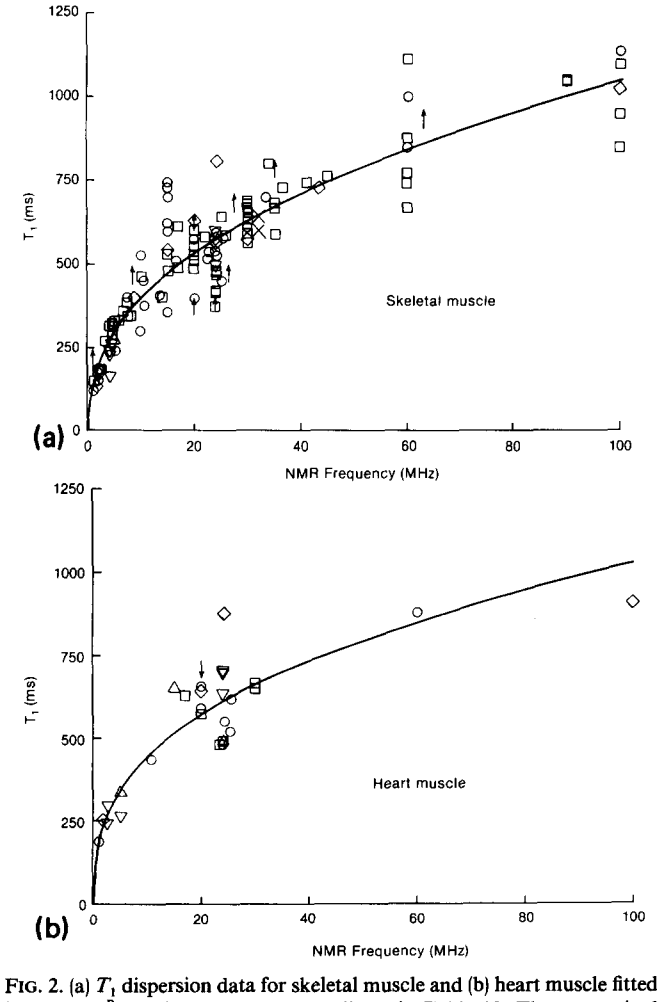

FIG. 2. (a) T_1 dispersion data for skeletal muscle and (b) heart muscle fitted to $T_1 = A\nu^B$. Fitting parameters are listed in Table 12. The mean cited standard deviation for each point expressed as a percentage of the T_1 value is about $(5 \pm 3)\%$.

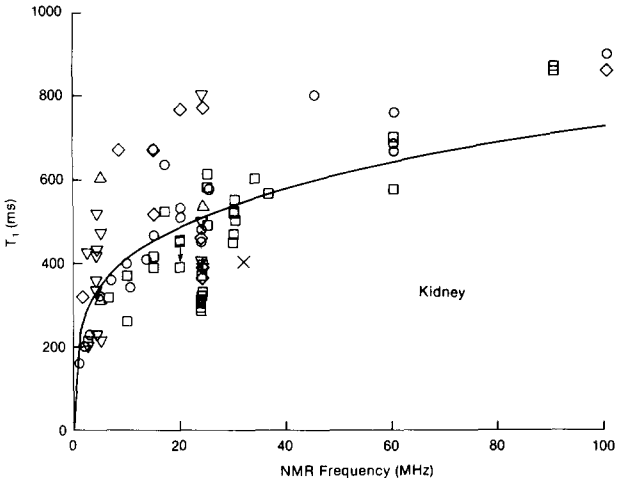

FIG. 3. T_1 dispersion data for kidney fitted to $T_1 = A\nu^B$ with parameters listed in Table 12. Cortex and medulla are undifferentiated. The mean cited standard deviation for each point expressed as a percentage of the T_1 value is about $(6 \pm 5)\%$.

group) were compared with tissues taken from an intact carcass (autopsy group), and excised tissue refrigerated overnight. No changes in T_1 greater than the experimental error (8%) were observable in any of these tissues, even after two days. The Goldsmith group observed no difference between autopsy and surgical rat muscle, liver, and lung T_1's and T_2's within experimental error (6%–16%). However, a 20% difference in colon T_1's was noted and attributed to intraperitoneal injection of anesthetic. In contrast, Beale implored researchers to "resist the temptation to place tissues on ice or in the refrigerator,"[8] but cited decreases in T_1 of only 8%, 8%, 18%, and 14% in muscle, breast, nipple, and lymph node, respectively, following 48 h refrigeration. Also Small *et al.*[145] measured up to a 30% decline in both long and short T_2 components of breast tissue following 24 h refrigeration, compared with the decrease of only 10% noted above with the samples kept at room temperature for the same period.

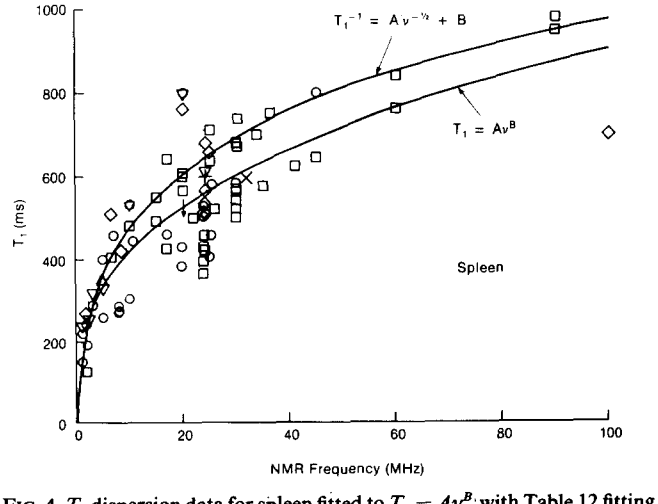

FIG. 4. T_1 dispersion data for spleen fitted to $T_1 = A\nu^B$ with Table 12 fitting parameters (standard deviation = 19%). A best fit to Escanye *et al.*'s equation,

$$T_1^{-1} = A'\nu^{-1/2} + B'$$

with $A' = 5036$, and $B' = 0.520$, gave a 21% standard deviation (Ref. 54). The mean cited standard deviation for each point expressed as a percentage of the T_1 value is about $(8 \pm 5)\%$.

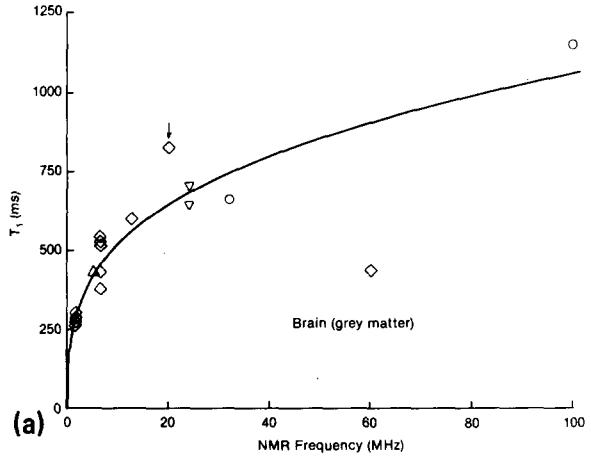

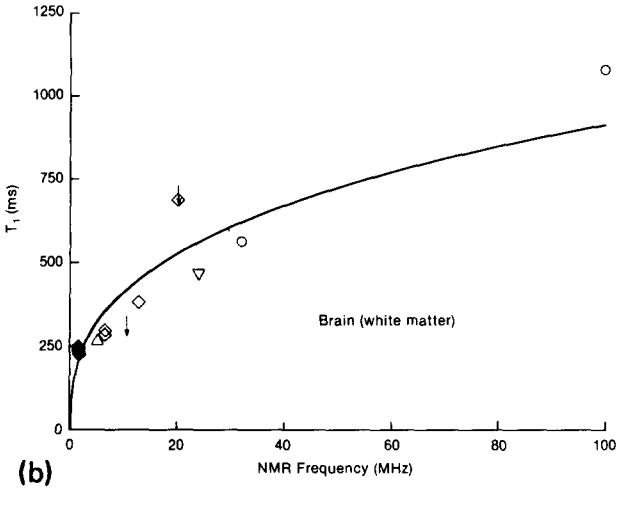

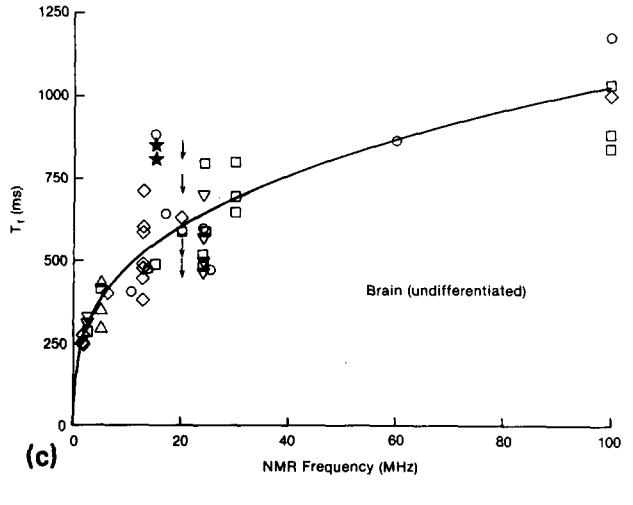

FIG. 5. (a) T_1 dispersion data for grey brain matter, (b) white brain matter, and (c) other undifferentiated brain tissue, fitted to $T_1 = A\nu^B$ with Table 12 fitting parameters. The mean cited standard deviation for each point expressed as a percentage of the T_1 value is about $(7 \pm 4)\%$.

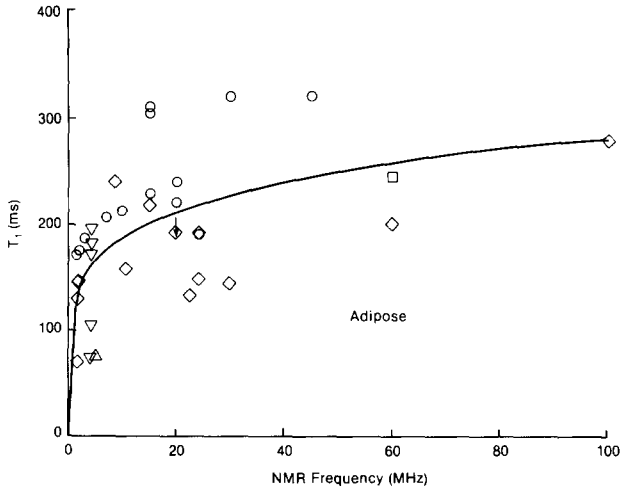

FIG. 6. T_1 dispersion data for adipose fitted to $T_1 = A\nu^B$ with Table 12 fitting parameters. The mean cited standard deviation for each point expressed as a percentage of the T_1 value is about $(12 \pm 6)\%$.

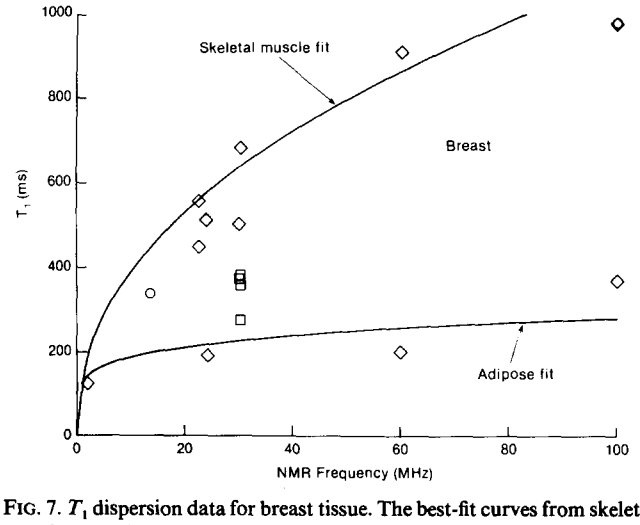

FIG. 7. T_1 dispersion data for breast tissue. The best-fit curves from skeletal muscle and adipose are superimposed for comparison. The mean cited standard deviation for each point expressed as a percentage of the T_1 value is about $(12 \pm 13)\%$.

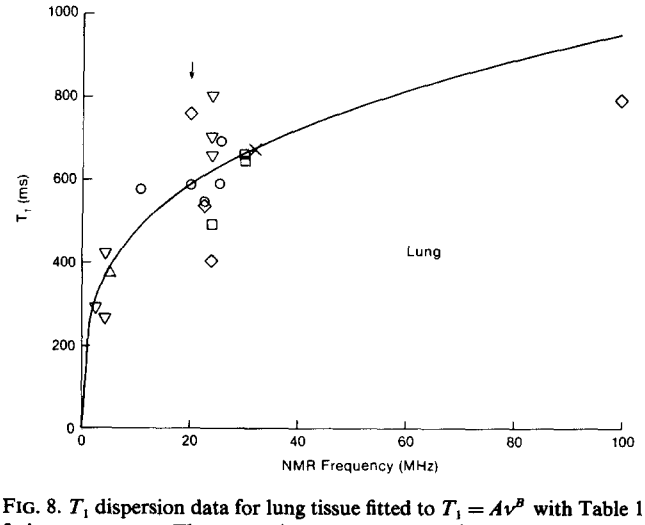

FIG. 8. T_1 dispersion data for lung tissue fitted to $T_1 = A\nu^B$ with Table 12 fitting parameters. The mean cited standard deviation for each point expressed as a percentage of the T_1 value is about $(10 \pm 10)\%$.

Table 12

MEAN ^{1}H TISSUE T_1 and T_2 RELAXATION TIMES

Tissue	T_1[1]			T_2[2]	
	A	B	SD(%)	T_2 (ms)	SD (ms)
Muscle					
skeletal	.000455	.4203	18	47	13
heart	.00130	.3618	16	57	16
Liver	.000534	.3799	22	43	14
Kidney[3]	.00745	.2488	27	58	24
Spleen	.00200	.3321	19	62	27
Adipose	.0113	.1743	28	84	36
Brain					
grey matter	.00362	.3082	17	101	13
white matter	.00152	.3477	17	92	22
unspecified	.00232	.3307	19	76	21
Lung	.00407	.2958	19	79	29
Marrow[4]				59	24
Breast[5]				49	16

1. $T_1 = A\,\nu^B \pm$ SD %, where ν = ^{1}H NMR frequency in Hz, SD = standard deviation expressed as a percentage of T_1, T_1 in sec.
2. Assumes T_2 is independent of frequency. Multicomponent data is omitted from the computations. T_2 is in ms. SD = standard deviation in ms.
3. Averages medulla and cortex.
4. Insufficient data for a T_1 fit.
5. Use skeletal muscle and/or adipose T_1 fits.

D. *In vitro* versus *in vivo* human measurements

In vivo relaxation time measurements from macroscopically homogeneous tissue types have arguably only become possible with the recent innovation of NMR imaging techniques. Tabulated ^{1}H human *in vivo* relaxation data are available only up to 15 MHz with grey and white brain matter having the most points. Figure 12 compares the human *in vivo* brain T_1 dispersions with the computed best-fit grey and white matter curves from Fig. 5. Note that data conform to the curves within the specified standard deviation (Table 12), and significant point scatter exists despite the constancy of species, temperature, tissue status, and averaged sample heterogeneity represented by the points. There may be a tendency for slightly elevated T_1 values measured *in vivo* compared to *in vitro* (see Sec. IV C), but such trends are concealed from the curve by the noise. For example, Gore *et al.*[70] and Ling and Foster[104] observe an approximately 13% decrease in the T_1's of muscle of dead intact rabbits compared to the living animals.

E. Dependence on age

Drastically elevated relaxation times are reported for neonatal tissue[30,77,94,96,97,103,114,148] persisting a few weeks in animals to at least several months after birth in humans. Hazlewood *et al.*[77] noted that immature muscle T_1 and T_2 (< 10 days old) were, respectively, 1.7 and 2.7-fold the mature values (> 40 days). They proposed that the fraction of "ordered water" increases during postnatal development. Similarly, Kiricuta *et al.*[96,97] reported immature rat brain, heart, and liver T_1 elevations of 110%, 50%, and 40%, respectively, attributable to an approximately 14% increase in water content in neonates compared to adults. Lewa and Zbytniewski[103] measured 8%–40% increases in the T_2's of liver, spleen, and skin in 3-month-old hamsters compared to 6-month-old animals. Buonnano *et al.*[30] observed that neonatal gerbil brain T_1's changed from 1.83 to 1.26 s in three weeks time after birth at which point "adult levels" are reached (Fig. 13). Misra *et al.*[114] recorded muscle T_1's of 1.24 s in 18-day embryo and 1-day postnatal chickens which declined to 0.746 and 0.647 s at 8 and 16 days postnatal, respectively (Fig. 13).

Some human fetal T_1's were tabulated by Kasturi *et al.*[94]: 0.721, 1.05, and 0.993 at 25 MHz for liver, lung, and kidney, respectively. These are about double the mean (adult) values plotted in Figs. 1, 8, and 3. Also Smith[148] noted "T_1 images of the neonatal brain (of a 9-week-old child) show a uniformly long T_1, due to the absence of myelin, and cannot differentiate between grey and white matter, the T_1 of both being markedly elongated at 390–400 ms" (at 1.7 MHz).

Evidence for relatively minor fluctuations in T_1 with circadian rhythm also exists. De Certaines *et al.*[46] observed a statistically significant 12% variation in rat liver T_1's excised as a function of time, with a peak at midday and minimum at dawn. No substantial corresponding fluctuations in either T_2 or water content were measured.

IV. COMPARISON WITH THEORY

A. Spin-lattice relaxation

The liquidlike ^{1}H T_1 frequency dispersions observed in biological tissue can involve both intramolecular and intermolecular dipolar interactions of macromolecules and water molecules of the general form

$$\frac{1}{T_1} = \frac{9}{8}\gamma^4\bar{h}^2[J^1(\nu) + J^2(2\nu)], \tag{3}$$

with $\gamma = 2.675\times10^8$ s^{-1} T^{-1}, $\bar{h} = 1.055\times10^{-34}$ Js, and where $J^1(\nu)$, $J^2(2\nu)$ are spectral density functions for the various motions evaluated at the resonance frequency and at twice that frequency.[1] Intramolecular processes involve mainly rotational motion with spectral density functions

$$J^1(\nu) = \frac{J^2(\nu)}{4} = \sum_{i,j}\frac{4C_{ij}}{15r_j^6}\left[\frac{\tau_{ij}}{1+4\pi^2\nu^2\tau_{ij}^2}\right], \tag{4}$$

where r_j is an intramolecular (H–H) distance between nuclear dipoles, C_{ij} are weighting coefficients independent of frequency, and the τ_{ij} are correlation times for the ith characteristic mode of motion of the jth intramolecular dipole pair.[1,57,64,98,159] Ignoring macromolecular hydrogen enables omission of the j summation so the r_j becomes the (fixed) separation between hydrogens in water molecules.

Many established models invoke two components of water in tissue undergoing rapid exchange relative to the NMR observation time: a large free water compartment and a bound water compartment hydrogen bonded to macromolecules or hydration layers.[38,47,54,55,57,60,61,75,92,96,98,140] The observation of a nonfreezing water component in many tissues,

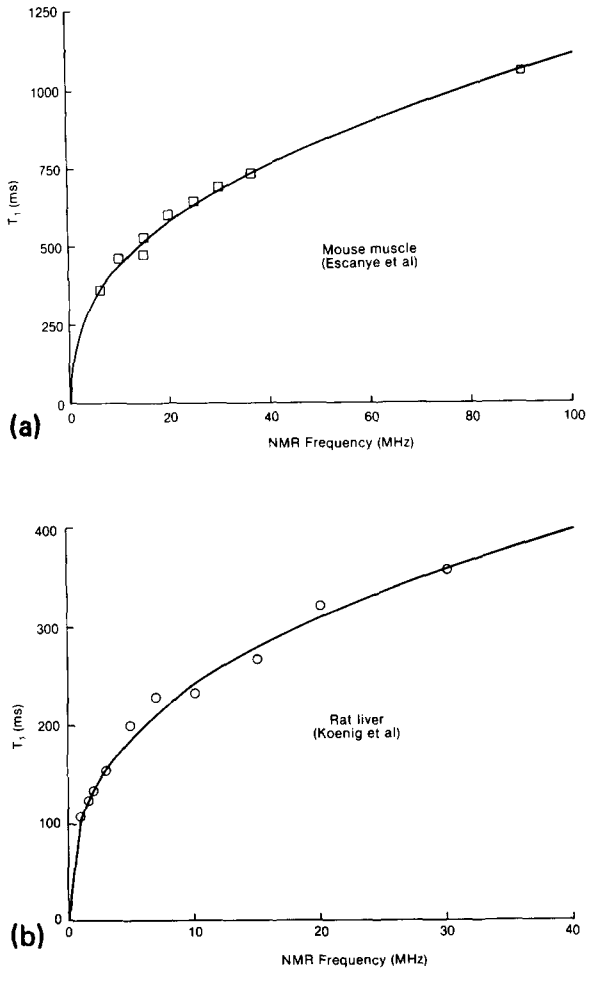

FIG. 9. (a) T_1 dispersion data for mouse muscle from Escanye *et al.* (Ref. 54), fitted to $T_1 = A\nu^B$ with $A = 0.000\,645$, $B = 0.4044$, and standard deviation 3.7%. The Escanye *et al.* fit,

$$T_1^{-1} = A'\nu^{-1/2} + B'$$

with $A = 6225$, $B = 0.300$ yielded the same standard deviation. (b) T_1 dispersion data for rat liver from Koenig *et al.* (Ref. 99) fitted to $T_1 = A\nu^B$ with $A = 0.000\,741$, $B = 0.3592$, and standard deviation 3.9%. The latter data were derived from relaxation rate curves and probably contains reading errors.

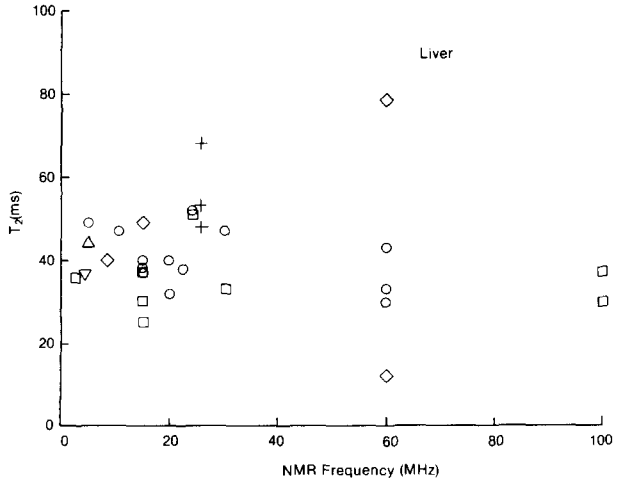

FIG. 10. T_2 dispersion data for liver omitting multicomponent measurements. The mean cited standard deviation for each point expressed as a percentage of the T_2 value is about (10 ± 10)%.

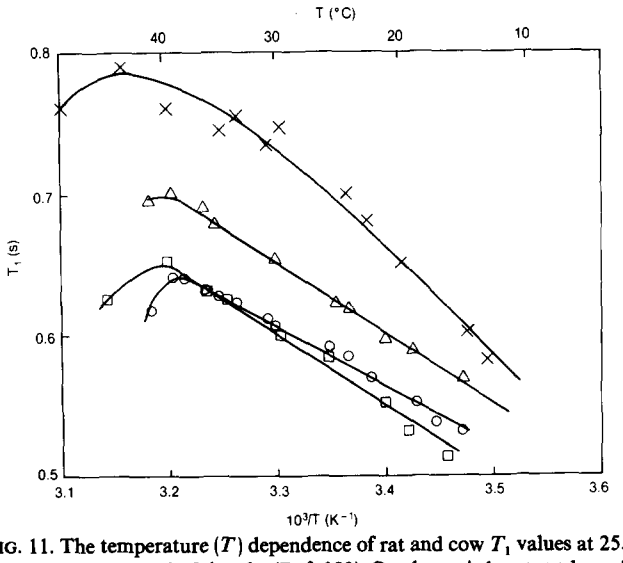

FIG. 11. The temperature (T) dependence of rat and cow T_1 values at 25.6 MHz from Lewa and Majewska (Ref. 102). ○ spleen; △ heart; × lung; □ muscle.

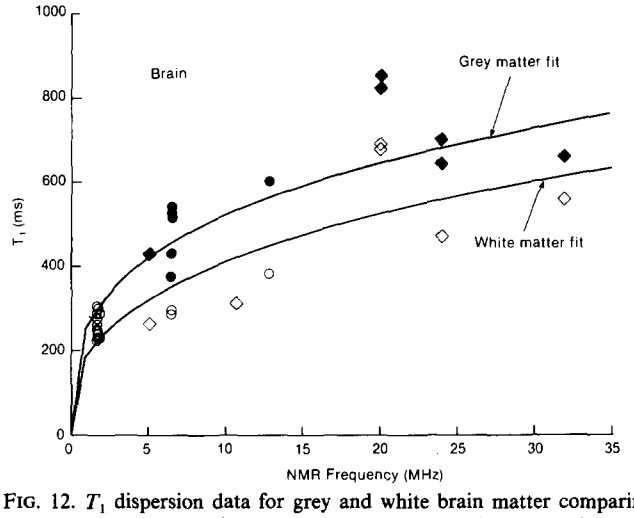

FIG. 12. T_1 dispersion data for grey and white brain matter comparing human *in vivo*, with all of the *in vitro* measurements. Circles and diamonds denote *in vivo* and *in vitro* data, respectively; shaded symbols correspond to grey matter. Curves of best fit from Figs. 5(a) and 5(b) are shown for comparison. The mean cited standard deviation for each point expressed as a percentage of the T_1 values are about (7 ± 4)%. ○ white matter *in vivo*; ● gray matter *in vivo*; ◇ white matter *in vitro*; ◆ gray matter *in vitro*.

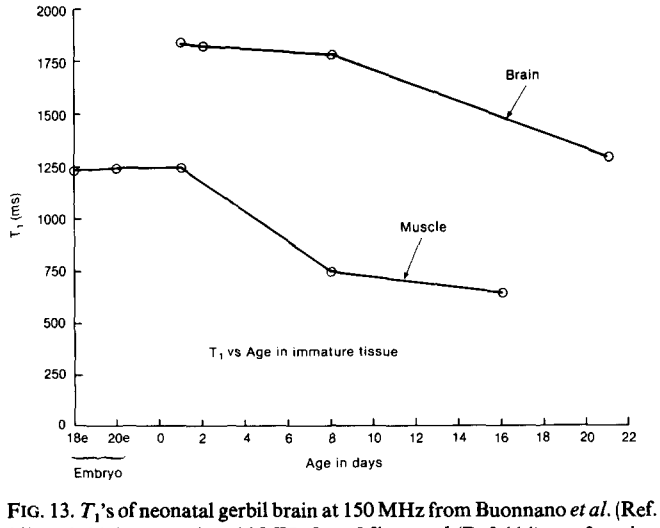

FIG. 13. T_1's of neonatal gerbil brain at 150 MHz from Buonnano *et al.* (Ref. 30), and chicken muscle at 20 MHz from Misra *et al.* (Ref. 114), as a function of age. The cited standard deviations for both data sets expressed as a percentage of the T_1 values is about 1%.

often directly identified with the bound phase, is key evidence for this FETS model.[111] A hypothesis, due to Ling, in which all intracellular water exists in an ordered, polarized state has also been invoked.[40,63,75]

The relaxation rate in the FETS model is a weighted average of the two states:

$$\frac{1}{T_1} \sim \frac{b}{T_{1b}} + \frac{1-b}{T_{1f}+\tau_e}, \tag{5}$$

where T_{1b} is the T_1 of the bound fraction ($b \ll 1$) of water, T_{1f} the T_1 of the free water fraction, and τ_e is the (short) residence time of water in the restricted compartment.[75,57] T_{1f} is approximately equal to the T_1 of tap water ($\sim$2–3 s) and constitutes $\sim$75%–99% of the total observed water ($b \sim 0.01$–0.25). Free water undergoes rapid translational and rotational diffusion, that is, $4\pi^2 \nu^2 \tau_f^2 \ll 1$ for $\nu \leqslant 100$ MHz with a single free water correlation time $\tau_f \sim 1$ ps. Thus T_{1f} is essentially independent of frequency. The frequency dependence of the measured T_1 is therefore determined by T_{1b}. That this is so for biological tissues is shown by T_1 experiments performed by Fung at 5, 30, and 100 MHz in which b is varied by soaking tissue samples in solutions of different osmolarity.[61,142] The extrapolated intercept from Eq. (5) is identified as $\sim 1/T_{1f}$ provided that $\tau_e \ll T_{1f}$, and corresponds to $T_{1f} \sim 1.7$ s independent of frequency.[61] Also Escanye *et al.*[54] determined

$$T_{1f} \sim 1.8 \begin{bmatrix} + & 1.3 \\ - & 0.5 \end{bmatrix} \text{ s}$$

independent of frequency from 6.7 to 90 MHz as a tissue average over normal and cancerous muscle, spleen, liver, and kidney. This results from equating Eq. (5) with their dispersion Eq. (2) wherein $B' \sim (1-b)/T_{1f}$.

The simplest model characterizes the rate $1/T_{1b}$ by isotropic rotational motion and a single correlation time, implying, from Eqs. (3)–(5), $T_1 \propto \nu^2$. Such behavior was fitted by Knispel *et al.*[98] to T_1 data measured over 17–45 MHz, but this model does not satisfactorily cope with the extended 1–100 MHz range investigated here.[54] Thus, multiple or continuously distributed correlation times are required. A dual correlation time model involving intramolecular interactions with anisotropic reorientation of bound water fitted Escanye *et al.*'s data,[54] but required excessive free water fractions in the range $0.98 \leqslant 1-b < 1$. Here, one correlation time would correspond to rapid motion about an axis perpendicular to the H–H direction, and the other to slow reorientation of this axis under the influence of macromolecular motion.[159]

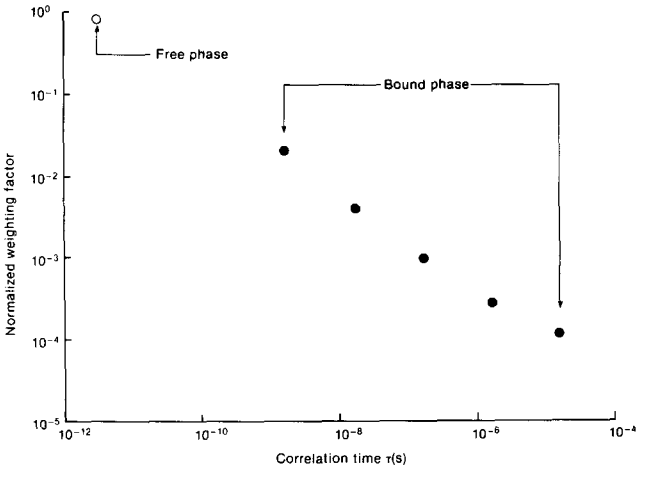

FIG. 14. Discrete distribution of six correlation times and their weighting factors fitted by Finch and Homer (Ref. 57) to frog muscle T_1 and $T_{1\rho}$ dispersions using Eqs. (3) and (4), and omitting the j-summation.

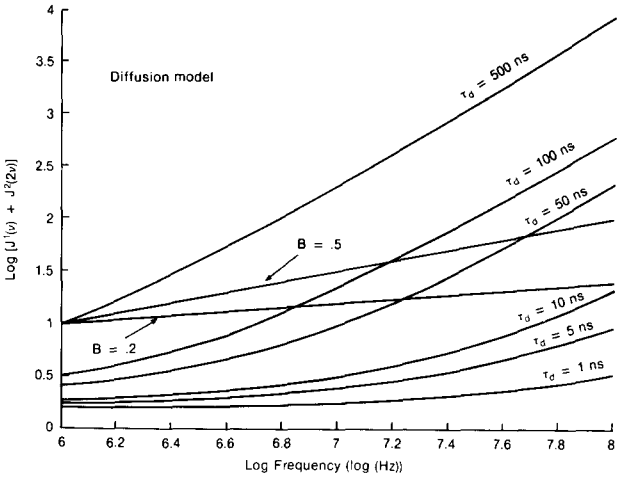

FIG. 15. Investigation of the isotropic diffusion model of T_1 relaxation in the bound phase (Ref. 54). The curves were obtained by numerical integration of Eq. (7) as a function of frequency from 1–100 MHz with different diffusion correlation times τ_d. Since

$$1/T_1 \propto J^1(\nu) + J^2(2\nu),$$

the model satisfies the empirical Eqs. (1) and (2) when a τ_d is found for which the curves are linear. Straight lines with gradients of 0.2 and 0.5 depict the actual range of B values observed (Table 12).

Whilst correlation times associated with intramolecular interactions are dominated by rotation, intermolecular interactions involve mainly translational motion. However, rotation and translation of water molecules in water are arguably coupled, suggesting that the same correlation times could be used to characterize both motions. This offers some justification for floating C_{ij} and r_j to intermolecular/intramolecular averages, and computing T_{1b} from Eqs. (3)–(5) with a single summation over the i correlation times.[57] Finch and Homer fitted such a model to frog muscle dispersion data to within experimental accuracy (5%), albeit using nine fitting parameters, including five discrete correlation times for the bound compartment and a single correlation time for the free compartment, and only 19 data points.[57] The resultant weighting coefficients (C_i) are plotted against correlation time in Fig. 14. The results appear consistent with the existence of several hydration layers bonded to macromolecules with increasing mobility in outer layers, and suggest a distribution of residence times (τ_e) rather than the single value assumed. However, the estimates of $(1-b)$ and τ_e seem somewhat excessive at 0.97 and 0.8 ms, respectively.

Models incorporating distributed correlation times for the molecular motion of the bound water fraction were proffered by Held *et al.*,[78] Fung and McGaughy,[64] and Escanye *et al.*[54] All attempted a log-Gaussian distribution function of intramolecular correlation times for rotation

$$g(\tau) = \frac{\alpha}{\tau\sqrt{\pi}} \exp\left\{ -\left[\alpha \ln \left| \frac{\tau}{\tau_0} \right|\right]^2 \right\}, \tag{6}$$

(α, τ_0 empirically determined constants), not dissimilar from the discrete distribution of Fig. 14, to provide a good fit to frog muscle frequency dispersion data recorded between 3 kHz and 75 MHz. This requires replacement of the Eq. (4) summation by the integral $\int g(\tau)d\tau$ which is then evaluated numerically,[64] again implicitly incorporating both intramolecular and intermolecular contributions by empirically fitting the parameters.

Escanye *et al.*[54] also proposed a model involving distributed correlation times to explain their fit to Eq. (2). In this model, T_1 relaxation is dominated by intermolecular interactions that consist entirely of translational diffusion of bound tissue water treated as spheres. The spectral density functions for isotropic, uniform translational diffusion are

$$J^1(\nu) = \frac{J^2(\nu)}{4} = \frac{M}{dD}\int_0^\infty [J_{3/2}(u)]^2 \frac{u\,du}{u^4 + 4\pi^2\nu^2\tau_d^2}, \quad (7)$$

where M is the ^{1}H spin density, $J_{3/2}(u)$ is a Bessel function of order 3/2, $u = rd$, r is the distance variable between diffusing molecules, d is the distance of closest approach, D is the diffusion coefficient and $\tau_d = d^2/2D$ is the diffusion jump time.[1,54] Assuming $d = 5$ Å and a 50-ns jump time, the model[54] yields a bound water diffusion coefficient of 2.5×10^{-8} $cm^{-2}s^{-1}$ that is about 400 times less than Hazelwood *et al.*'s bulk muscle tissue measurements.[75,74] However, the latter must be considered as free/bound fraction averages. Alternatively, Koenig *et al.*[99] used the heuristic Cole–Cole expression

$$\frac{1}{T_1} = \frac{1}{T_{1f}} + G + \frac{H\,[1 + (\nu/\nu_c)^{\beta/2}\cos(\pi\beta/4)]}{1 + 2(\nu/\nu_c)^{\beta/2}\cos(\pi\beta/4) + (\nu/\nu_c)^{\beta}}, \quad (8)$$

where G, H, ν_c, and β are four fitting parameters to be determined.

Semiempirical multiparameter models such as these are susceptible to the criticism that given enough variables, success is virtually guaranteed, particularly since the experimental dispersions are apparently continuous, slow varying, and monotonic. Close scrutiny of predicted parameters is necessary to determine their physical relevance. Thus the relation, $T_1 = A\,\nu^B$, allowing the exponent to vary empirically, provides as good or better average fit to the tabulated data as the Escanye group's equation (Figs. 1 and 4), and an excellent, if not superior fit to the individual tissue dispersions of Escanye *et al.* and Koenig *et al.* (Fig. 9) with minimal fitting coefficients compared to Eq. (3)–(8). Although its physical significance is yet to be determined, the resemblance of Eq. (1) to the Escanye *et al.* isotropic diffusion model and Eq. (2) is undeniable. However, numerical evaluation of Eqs. (3) and (7) using similar values of τ_d, d, and D yields curves nonlinear in $\log(T_1)$ versus $\log(\nu)$ over 1–100 MHz, contrary to the requirements of both Eqs. (1) and (2) (Fig. 15). Therefore, either a distribution of diffusional correlation times are necessary, or intramolecular rotational contributions cannot be totally neglected.

Estimates of the relative importance of the intermolecular and intramolecular mechanisms to bound water relaxation are open to ambiguous interpretation. *A priori*, the r_j^{-6} dependence of the dipole–dipole interaction [Eq. (4)] strongly favors dominance by intramolecular processes. However, both intermolecular and intramolecular models can be fitted to the T_1 dispersions with essentially equivalent ease or difficulty because both contain terms quadratic in frequency [compare Eqs. (4) and (7)]. To elucidate the relative importances of the two mechanisms, Civan and Shporer,[37] and Fung[62] observed the ^{1}H T_1's at 4.3, 8.1, and 35 MHz of muscle and brain tissue bathed in various concentrations of deuterated water (^2H_2O) in Krebs or Ringers solution for 1–3 h. Since the gyromagnetic ratio of ^{2}H is 0.15 that of ^{1}H, the substitution of ^2H_2O for ^1H_2O in bulk water reduces the strength of intermolecular H_2O–H_2O dipolar interactions for ^{1}H. It also reduces the intramolecular H–H dipolar interaction since ^1H_2O and ^2H_2O undergo rampant chemical exchange to $^1HO^2H$. Thus, bulk water T_1 rapidly increases as the ratio $[^2H_2O/^1H_2O]$ increases. In tissue, the increase is much less: about 20% extrapolating to complete substitution compared to a factor of 24 for bulk water. Rustgi *et al.*[140] extended these measurements over the frequency range 15–60 MHz for muscle tissue, recording essentially the same observation.

This somewhat surprising and significant result is interpreted as evidence that tissue ^{1}H relaxation is dominated by intermolecular interactions between macromolecules and water molecules in the first hydration layer. This is the only remaining relaxation mechanism that is transparent to the ^2H_2O substitution.[62] The small 20% change observed is possibly attributable to chemical exchange between macromolecular and water hydrogens. The implication is that tissue T_1 relaxation entirely hinges on the interaction between macromolecules and a single adsorbed layer of water. The relaxation mechanism may be either translational or rotational and likely involves the stronger H–H interactions. To explain the dispersion data, a distribution of correlation times in the neighborhood ~ 10 ns is necessary. If the interaction is principally translational, as in the Escanye *et al.* model, then the residence time τ_e also cannot be much longer than 10 ns.

B. Spin–spin relaxation

An expression for the T_2 dispersion corresponding to Eq. (3) is

$$\frac{1}{T_2} = \frac{3}{4}\gamma^4\bar{h}^2\left[\frac{3}{8}J^0(0) + \frac{15}{4}J^1(\nu) + \frac{3}{8}J^2(2\nu)\right], \quad (9)$$

where $J^0(0)$ is the static component of the spectral density functions[1] and includes here effects due to microscopic and molecular level field heterogeneity in biological tissue. Thus T_2 is independent of frequency if the latter two terms in Eq. (9) are small compared to the first, static contribution. The similarity of structure of these terms with Eq. (3) ensures the frequency independence of T_2 if T_2 is much less than T_1. This is true of virtually all of the (nonfluid) tissues, except perhaps for the longest of the liquidlike (L) multiple components of T_2, and for adipose whose T_1 dispersion is essentially constant above 10 MHz anyway. The dispersions of long T_2 components are more likely to follow those of the corresponding T_1's. Like T_1, T_2 can also be equated to a sum of contributions from free and bound components in an expression analogous to Eq. (5). The static intramolecular spectral

density function due to rotation is $J^0(0) = 6J^1(0)$ in Eq. (4), and the static intermolecular spectral density function, due to isotropic translational diffusion, is

$$J^0(0) = 2N/15dD = 2\pi N\eta/5kT$$

where η is the viscosity and k is Boltzmann's constant.[1]

Evidence for multicomponent relaxation times is less compelling for T_1 than for T_2. The sparse multicomponent T_1 data reported are largely explicable by sample or chemical heterogeneity. For example, in adipose tissues, ^{1}H chemical shift spectroscopy reveals two principal components associated with H_2O and $-CH_2-$ (macromolecular) hydrogens[23] with different T_1 and T_2 relaxation times thus far neglected in the above analysis. Breast and other tissues with large fatty components, high blood content, or other heterogeneity such as grey and white brain matter, or kidney cortex and medula can easily yield multicomponent relaxation values. Multicomponent T_2's that are not attributable to macroscopic or microscopic heterogeneity are difficult to explain at a molecular level. Given the similarity of mechanisms responsible for T_1 and T_2 relaxation, can multicomponent T_2's coexist with single-valued T_1's?

Hazlewood, Chang, and colleagues interpreted the multicomponent T_2 data as evidence against the fast exchange model.[34,75] However, slow exchange would require residence times τ_e of the order T_2 ($\sim$10 ms), which could be expected to generate observable multicomponent T_1 data. Diegel and Pintar responded that the different behavior is explicable via the static T_2 spectral density term.[47] They observed dual component tissue $T_{1\rho}$'s (effectively, the T_1 at extremely low frequency) from $\sim$0–60 kHz equivalent to the T_2 values and attributed to intercellular (150 ms) and intracellular (53 ms) water. The faster low-frequency $1/T_{1\rho}$ and $1/T_2$ relaxation rates can be accounted for by a $\sim 10\,\mu$s correlation time identified with the residence time τ_e for diffusion of water in the hydration layer.[47,98] This exchange diffusion is too slow to directly effect T_1 relaxation between 1–100 MHz, but, since $\tau_e \ll T_1$, it strongly averages the different T_1 values from the various compartments leaving the observed T_1 single valued in the >1 ms range. $T_{1\rho}$ measurements in normal and deuterated muscle, spleen, and kidney by Rustgi *et al.*[140] confirm the importance of exchange diffusion as a relaxation process at extremely low frequencies. The exchange diffusion can directly effect tissue water T_2's by exposing water molecules to static field inhomogeneities at the exchange interface: Fung and McGaughy[64] note microscopic field inhomogeneity as a likely explanation why $T_2 < T_1$ in tissue.

This model is incompatible with the Escanye *et al.* view of T_1 dispersions in the 1–100 MHz range dominated by diffusion, since it would require $\tau_e \sim \tau_d$, but is compatible with the rotational modeling of T_1. The free water correlation time is still ~ 1 ps, much faster than both the exchange correlation time $\tau_e \sim 10\,\mu$s and the suggested distribution of rotational correlation times τ in the range 10 ns responsible for T_1 relaxation.

Some additional information on multicomponent T_2's is provided by Peemoeller *et al.*[128] who analyzed the relative contributions of water and macromolecular hydrogens to each component in mouse muscle by comparison with tissue soaked in an osmotically balanced ^2H_2O solution for 4 h. They ascribe a 143 ms (L) and a 24 μs (S) T_2 component to macromolecules, a 40 ms (SL) component to water alone, and a 5 ms (SS) component to both water (70%) and macromolecules (30%). This is a more likely allocation of T_2 components than the Diegel and Pintar intercellular/intracellular assignment,[47] and is consistant with the aforementioned observation of discrete H_2O and $-CH_2-$ peaks in some tissue ^{1}H NMR spectra.[23] Aside from the possibility of chemical exchange, macromolecular components cannot be expected to participate in fast exchange.

C. Temperature dependence

The relaxation times depend on temperature via the rotational and translational correlation times τ_i and τ_d. Setting

$$\tau_i = \tau_{i0} \exp(E_{ia}/kT) \tag{10}$$

for the bound water hydrogens in Eqs. (3)–(7) and (9), where τ_{i0} and E_{ia} are, respectively, a constant and the activation energy for the ith mode of motion,[1] could precisely define the temperature dependence of the relaxation times if indeed the relaxation time model were precisely understood. Assuming the bound fraction b is temperature independent, then in the limit $2\pi\nu\tau_i \ll 1$ the frequency-dependent denominators of the rotational spectral density functions [Eq. (4)] approach unity, and substitution of Eq. (10) in Eqs. (5) and (3) gives

$$T_{1f} \sim \exp(-E_{af}/kT) \text{ and } T_{1b} \sim \exp(-E_{ab}/kT), \tag{11}$$

or more crudely,

$$T_1 \sim \exp(-E_a/kT),$$

where E_{af}, E_{ab}, and E_a are activation energies for the T_{1f}, T_{1b}, and T_1 processes. This dependence is assumed by Lewa and Majewska[102] and Parker *et al.*[125] to explain their observed linear behavior of T_1 with temperature. It should also describe the T_2 temperature dependence when the static spectral density term is dominant. For small temperature variations, the series expansion for exponentials suggests an approximately linear relationship between T_1 and $1/T$, with T_1 increasing with increasing temperature. Furthermore, if the reorientation is random, then Stokes' formula $D_r = kT/8\pi a\eta$ for the rotational diffusion coefficient of spheres, where a equals the molecular radius, provides $\tau_i = 4\pi\eta a^3/3kT$, instead of Eq. (10). Thus the same result $T_1 \propto 1/T$ obtains directly.[1,19] In models dominated by translational diffusion, application of Stokes' formula $D = kT/3\pi d\mu$ (so $\tau_d = 3\pi d^3\,\eta/2kT$) for the translational diffusion coefficient to Eqs. (7) and (3) repeats this result.[1,19] Since absolute temperature changes relatively little between 0 and 40 °C, T_1 also varies roughly linearly with T. Extending the temperature range beyond this risks irreversible structural transitions in tissue not representative of the physiological state.[102]

The small temperature range and the relatively modest variations in the observed T_1's so induced, are likely responsible for the success of these simple formulations for the temperature dependence, despite the somewhat dubious assumptions. Moreover, to explain the experimental tissue T_1 dispersions requires $2\pi\nu\tau_i \gtrsim 1$ for the dominant relaxation processes[54] in models employing Eqs. (4) or (7), thereby

modifying the above proportionalities and introducing frequency dependence to the temperature dependence. Indeed, under this condition, the denominators of Eqs. (4) and (7) predominate, and application of either Stokes' formulas or Eq. (10) anticipates a decreasing T_1 with increasing temperature, contrary to the data. The dilemma is resolved in the T_1 model employing a log-Gaussian distribution of correlation times by incorporating temperature dependence into the distribution function parameters [Eq. (6)] via $\alpha = \alpha_0 \sqrt{T}$, and

$$\tau_0 = \tau_{0\infty} \exp(E_a/kT),$$

where α_0 and $\tau_{0\infty}$ are constants.[63,64] Fung and colleague's simultaneous fitting of muscle and liver T_1 dispersion data from 4.5 to 60 MHz over -70 to 40 °C utilizing this model is persuasive evidence for its validity.

The observed increase in the derivative of T_1 with respect to temperature ($\partial T_1/\partial T$) with increasing frequency is an important feature of the data, consistent with the distributed correlation times of Fung *et al.*'s model. In fact, since the temperature-dependent correlation times appear as coefficients of the frequency dependent terms in Eqs. (4) and (7), Eq. (1) might suggest $\partial T_1/\partial T \sim \nu^B$ with $B \sim 1/3$. Thus an eightfold frequency change from 7.5 to 60 MHz could result in an approximately twofold increase in the temperature dependence, in fair agreement with Fung *et al.*'s observation on mouse muscle and liver,[62] and the 20-fold increase in frequency between 1–20 MHz studied by Koenig *et al.* might account for a threefold increase in temperature dependence in approximate agreement with their rabbit blood data.[99] However, above 20 MHz the magnitude of the difference between T_1 values measured at room temperature and at physiological temperature is unresolved due to the dearth of physiological temperature data from all tissues except Fung *et al.*'s muscle and liver data. If the larger temperature dependences noted by Fung *et al.* were generally applicable, then the tissue curves (Figs. 1–9) could seriously underestimate the high-frequency behavior of the *in vivo* T_1 values. Below 20 MHz, the consensus from the tables and *in vivo* versus *in vitro* plot (Fig. 12) is that temperature differences between 20 and 37 °C do not significantly affect the T_1 values of nonfluid tissues.

The slight increase in T_2 with decreasing temperature observed by Belton *et al.*[14] is consistent with the role of the exchange process as a T_2 relaxation mechanism,[14,47] transparent to T_1 processes except for the mixing of free and bound values. As the temperature decreases, exchange slows and contributes less to T_2 relaxation so that T_2 initially increases.[14] Eventually T_2 decreases as other molecular motions slow with further declines in temperature. No frequency variations in tissue T_2 temperature dependence over 1–100 MHz are anticipated in view of the apparent frequency independence of T_2.

D. Tissue, species, and age dependence

The ^{1}H tissue water relaxation times measure molecular level structure and motion and therefore depend on the organization and composition of the tissue. Investigations of the correlation between T_1 and tissue water content are legion.[6,26,36,43,46,61,76,80,86,87,92–94,96,104,108,127,130,133,134,142,144] The mean fractional water contents by weight of normal rat and mouse liver, kidney, spleen, muscle, brain, and adipose tissue are 0.69 ± 0.01, 0.74 ± 0.01, 0.77 ± 0.02, 0.75 ± 0.02, 0.79 ± 0.01, 0.18 ± 0.03, respectively, averaged from Refs. 26, 43, 46, 76, 80, 86, 87, 92, 96, 97, 130, 134, 142, and 144. These correlate directly with T_1: the higher the water content, the longer the T_1, prompting Mansfield and Morris[111] to write for a (nonadipose) tissue with fractional water content w

$$T_1 = 7.94\, w - 5.16, \tag{12}$$

assuming Kiricuta *et al.*'s 60-MHz rat data.[96] This relation emphasizes the observation that quite marginal changes in w are associated with large variations in T_1. In fact, the changes in w with respect to T_1 are so marginal that the physical significance of the correlation between T_1 and water content alone is doubtful.[108,133] Differences in macromolecular composition and structure, which could well influence the amount and motion of adsorbed water molecules and indeed the total tissue water content, thus probably constitute the primary source of variations in T_1 amongst different tissue types.

A remarkable feature of the relaxation data is its apparent independence of species. From the NMR standpoint, a human muscle is a rat muscle is a pig muscle is a frog muscle is a chicken muscle, etc., notwithstanding potential variations due to temperature. Again composition and structure are possible causes. Mansfield and Morris[111] tabulate human tissue water contents that are 2% to 7% higher than the rat/mouse averages cited above. In view of Eq. (12), these differences are too significant to permit the species independence of relaxation times, suggesting that water content is not directly responsible for the species' similarities amongst relaxation times. Macromolecular composition and structure are important to tissue function as well as to the relaxation times. Thus once the function has evolved, differences amongst species are apparently only of secondary importance at the molecular NMR level. Alternatively, it is possible that the differences in water content cited reflect systematic differences in the methods of measurement of water content.

Mansfield and Morris[111] also note a 2.5% per decade decline in human body water content from ages 40 to 70, which should dramatically reduce the corresponding T_1's if Eq. (12) were a determining influence. Subject age is a widely neglected parameter in human studies that could potentially create chaos of efforts to develop normal ranges of T_1, should significant variations occur. For immature tissue, large elevations in T_1 (Fig. 13) do correlate with increased water content, yet the possible role of macromolecular structural development as the principal determining factor again cannot be ruled out.

V. ERROR AND OMISSIONS

While evidence for the dependence of tissue relaxation times on temperature, time after excision, *in vivo* versus *in vitro* status, time of day, age, and species exists, these factors are demonstrably not entirely responsible for the scatter amongst T_1 and T_2 tissue dispersions. Other possible factors

are inherent tissue heterogeneity, sample handling techniques, the NMR measurement methods, the existence of multiple T_2 components, as well as presently unidentified sources. Tissue heterogeneity is unlikely to significantly influence scatter because of the large number of samples typically studied and the relatively small standard deviations quoted for individual T_1 points. Sample handling is a key issue for *in vitro* studies, addressed in depth by Beall.[8] We recommend that investigators perform measurements as soon as possible after death and excision, and that measurements for *in vivo* comparison be performed at physiological temperatures with samples that have not been overheated, frozen, homogenized, soaked, dehydrated, or otherwise abused.

The reviewed *in vitro* T_1 measurements were performed by either inversion recovery, or by partial saturation, or saturation recovery, or in one case by rapid ramping of the field,[99] or by the less accurate null method. The few investigators that employed the null technique almost invariably verify experimental accuracy by comparison with measurements obtained by the other methods. *In vitro* T_2 measurements were performed mainly by the standard Carr–Purcell or Carr–Purcell–Meiboom–Gill methods. Therefore, we could not objectively discriminate against T_1 and T_2 data on the basis of measurement technique, nor were there sufficient grounds to exclude data due to sample handling transgressions, except where stated in the Sec. II.

Perhaps the most dubious practices abound in the measurement of relaxation times, particularly T_2, *in vivo* utilizing NMR imaging techniques. To expedite patient scan times, T_1 and T_2 measurements are typically performed using only two points on the nuclear magnetization relaxation curves for each image picture element.[32,33,44,45,49,70,79,82,83,88,109,110,116,117,139,148–152,158] Unfortunately, the standard expressions employed for computing T_1 from inversion or saturation recovery presume precise 90° or 180° radiofrequency (rf) NMR pulses at each picture point across the image plane,[51] a difficult task for conventional NMR transmitter coil designs. The effect is dramatically illustrated by Gore *et al.*,[70] who reported T_1 variations of up to 60% from the same sample as a result of increasing the relaxation recovery time t from 0.2 to 0.4 s. They attributed the variations to multiple-component T_1 behavior which our review deems unlikely. A prudent approach to accurate T_1 measurement in the presence of inhomogeneous rf fields in NMR imaging is to use a three-parameter fit to the signal intensity

$$S = P + Q\exp(-t/T_1), \tag{13}$$

where P, Q, and T_1 are fitting constants.[56] Obviously, more than two data points would be required.

The situation is worse for *in vivo* T_2 studies since multiple components are widely identified *in vitro*. Hence, Gore *et al.*[70] tabulated variations in T_2 of up to 350% comparing values from the same sample computed from spin echoes occurring at 32 and 64 ms after the initial 90° rf pulse. Furthermore, the pulsed gradient spin-echo imaging experiment employed in T_2 imaging studies is a facsimile of the standard Stejskal and Tanner pulsed gradient diffusion measurement technique.[153] Since bulk tissue diffusion coefficients are significant fractions of pure water values,[74,75] attenuation of computed T_2's by diffusion effects is quite predictable. Diffusion and ignorance of multiple components may thus substantially account for the sad state of the T_2 data. If dual-point T_1 and T_2 imaging measurements become convention, and if the resultant T_1 and T_2 values are to be useful as diagnostic parameters independent of the particular imaging system and suitable for comparison, then standardized image sequence timing parameters should be adopted and any rf inhomogeneity problems solved.

The sparsity of relaxation data above 30 MHz and the absence of *in vivo* data above 15 MHz are additional deficiencies, although we certainly do not claim to have found all of the published measurements.

VI. CONCLUSIONS

The principal determinants of T_1 relaxation in normal biological tissue in the range 1–100 MHz are NMR frequency (ν) and tissue type. All of the tissue T_1 dispersions studied obey the simple relationship $T_1 = A\nu^B$, where A and B are parameters dependent on tissue type and $B \sim 1/3$. This expression gives an equivalent or better fit to T_1 data than previously used expressions and models and is simple enough to enable rapid computation of T_1 values at any desired frequency between 1 and 100 MHz. The standard deviations of T_1 from the fitted curves are about 20% reflecting mainly systematic errors not readily identifiable with species, temperature, *in vivo* versus *in vitro* status, time after excision, or age differences. Fetal and immature tissue excluded from this analysis exhibit dramatically elevated T_1 values. Most data are recorded at room temperature or physiological temperature, but there is a dearth of the latter measurements above 20 MHz. Evidence that the temperature dependence of T_1 increases significantly at higher frequencies could, therefore, result in our mean curves underestimating the high-frequency physiological temperature data. Virtually all researchers report single component T_1 values. However, breast tissue T_1 dispersions can be resolved into two components comprising adipose and fibrous tissue which have essentially equivalent dispersions to those of skeletal muscle and adipose. Dual components can arise from macroscopic tissue heterogeneity or from the discrete chemical species H_2O and $-CH_2-$ on macromolecules when these are sufficiently mobile to be detectable on the time scale of the NMR experiment.

The principal determinant of T_2 relaxation in normal biological tissue in the range 1–100 MHz is tissue type. No substantial dependence on NMR frequency, temperature, *in vivo* versus *in vitro* status, time after excision, or age can be differentiated within systematic errors of about 30%. Therefore average T_2 values are tabulated as constants for each tissue. Substantial evidence for multiple T_2 components exists. In muscle, the major component ($T_2 \sim 40$ ms), constituting about 75% of the signal, derives from tissue water. There exist very long ($T_2 \sim 140$ ms) and very short ($T_2 \sim 20\ \mu$s) T_2 components from macromolecules contributing about 7% and 11% each, and a short T_2 component ($T_2 \sim 5$ ms) of about 7% derived from both water and macromolecules. Multicomponent T_2's and diffusion in the presence of imag-

ing gradients are deleterious factors affecting *in vivo* T_2 measurements which must be dealt with.

The observed tissue T_1 and T_2 relaxation data can be substantially accounted for by the FETS model with free and bound phases of water undergoing rapid exchange. There is disagreement concerning the detailed mechanisms responsible for relaxation, however we tentatively offer the following scenario consistent with the reviewed data and which incorporates elements from the models of Fung *et al.*, Diegel and Pintar, Rustgi *et al.*, and the results of the deuterated water exchange experiments of Fung, Rustgi *et al.*, Civan and Shporer, and Peemoeller *et al.*

Water in the free phase undergoes rapid, probably correlated, rotational and translational motion with a correlation time of order 1 ps. This is too fast to directly affect relaxation between 1 and 100 MHz so the T_1 of the free phase is long ($T_{1f} \sim 1.7$ s) like ordinary water and independent of frequency. In muscle, the bound phase constitutes about 10% of the total tissue water content and consists of a single hydration layer adsorbed on the surface of macromolecules. The intramolecular rotational correlation time of these water molecules is probably still about 1 ps, but faster relaxation of water hydrogen is facilitated via intermolecular interactions involving mainly macromolecular hydrogen. The latter mechanisms requires a log-Gaussian or similar distribution of correlation times for motion, probably rotational, in the NMR frequency range, of order 10 ns. This faster intermolecular relaxation process is primarily responsible for the observed T_1 frequency, temperature, tissue type, and age dependencies. The bound water undergoes exchange diffusion with the free component with a slower correlation time of about 10 μs, which may be identified as the residence time in the bound state. The exchange diffusion correlation time is too long to facilitate T_1 relaxation directly but could provide an important relaxation mechanism for $T_{1\rho}$ and T_2. Nevertheless, it is sufficiently short to prohibit resolution of the free and bound water T_1's on the time scale of the T_1 experiment. Thus the observed water T_1 relaxation rate ($1/T_1$) is essentially equal to the sum of the free and bound water relaxation rates.

Unlike T_1, T_2 largely measures the low-frequency and static components of molecular motion and can therefore discriminate free and bound water and macromolecule phases. The bound water and the corresponding macromolecular adsorption surface must share the same low-frequency or static motional environment and can therefore be assigned the joint short T_2 component of about 5 ms in muscle. The major free water component exhibits a unique, significantly longer T_2 value ($\sim$40 ms in muscle) reflecting its greater mobility. However the free water component T_2 value is much less than the free water T_1 values ($\sim$500 ms) owing to an exchange diffusion relaxation mechanism. Thus, the free water component T_2 relaxation rate ($1/T_2$) is equal to the sum of the rate due to exchange diffusion at the exchange interface, and the much slower rate in the true liquid water phase. The exchange diffusion rate decreases with decreasing temperature, causing the free water component T_2 to increase slightly. Since this is the major component, and T_2 varies with tissue type, the exchange diffusion correlation time is likely tissue dependent. A physical candidate for the exchange diffusion relaxation mechanism is local static field gradients between the exchange interface and the free phase due to the presence of the macromolecules. The remaining two macromolecular T_2 components have no water counterparts. The extremely short component around 20 μs probably corresponds to rigid membrane or protein structures not normally observable in the NMR experiment, and the very long 140-ms component to highly mobile hydrogen on fatty acids, with essentially no hydration layer. The dominant role of low-frequency relaxation mechanisms for all T_2 components except the very long component ensures T_2 dispersions independent of the NMR frequency. The 140-ms fatty acid T_2 component may be associated with the comparably valued T_1 observed in adipose tissue, in which case its frequency dispersion will be similar.

Further effort is necessary to evaluate the full range of fitting parameters for the model peculiar to each tissue, and to tighten the uncertainty of the normal T_1 and T_2 values. It is imperative that guidelines be established for reproducible measurement of tissue NMR relaxation *in vivo*.

Note added in proof: Koenig *et al.*[162] recently published ^{1}H T_1 dispersions of normal and partially deuterated rat tissue from 10 kHz to 100 MHz. The Fung and Rustgi *et al.* observations on deuterated tissues are confirmed over 1–100 MHz. Koenig *et al.* attribute the 1–100 MHz dispersions to intermolecular interactions at the macromolecule–water interface. Below 1 MHz the difference between the normal and partially deuterated tissue T_1 increased to twofold at 10 kHz, indicating the increasing role of intra- (and possibly inter-) molecular H_2O–H_2O interactions at low frequencies. These observations are consistent with our best-guess model. Slight structure ($\sim$6% T_1) was observed in the heart muscle dispersions between 2 and 3 MHz and attributed to magnetization transfer (cross relaxation) between H_2O and ^{14}N nuclei on protein amides. A similar effect is noted in leeches by Kimmich *et al.*[163]

Bakker and Vriend[164] published statistically significant dual-component excised mice fat, kidney, muscle, and spleen tissue ^{1}H T_1's at 60 MHz. Except for fat, results showed a short component of 2–10 ms constituting 5%–8% of the magnetization, and a long component of comparable value of those cited herein. Dual components are attributed to the use of long (150 μs) 180° rf pulses in an inversion recovery sequence combined with a mechanism of ^{1}H–^{1}H cross relaxation[165] between H_2O and macromolecules at the interface.

ACKNOWLEDGMENTS

We thank W. A. Edelstein for modifying our least-squares fitting routine to minimize the fractional T_1 differences, R. W. Redington for scientific support, and the staff of the Research Center's Whitney Library for locating publications.

[1] A. Abragam, *The Principles of Nuclear Magnetism* (Oxford University, London, 1978), pp. 291–303.
[2] T. Araki, T. Inouye, T. Matozaki, and M. Iio, in *Proceedings of the 2nd Annual Meeting of the Society of Magnetic Resonance in Medicine* (Society of Magnetic Resonance in Medicine, Berkeley, CA, 1983), pp. 3–4.

[3]D. R. Bailes, I. R. Young, D. J. Thomas, K. Straughan, G. M. Bydder, and R. E. Steiner, Clin. Radiol. **33**, 395 (1982).
[4]C. J. G. Bakker and J. Vriend, Phys. Med. Biol. **28**, 331 (1983).
[5]L. E. Barroilhet and P. R. Moran, Med. Phys. **2**, 191 (1975).
[6]P. T. Beall, in *Proceedings of the 2nd Annual Meeting of the Society of Magnetic Resonance in Medicine* (Society of Magnetic Resonance in Medicine, Berkeley, CA, 1983), pp. 28–29.
[7]P. T. Beall, Magn. Reson. Imag. **1**, 189 (1982).
[8]P. T. Beall, Magn. Reson. Imag. **1**, 165 (1982).
[9]P. T. Beall, Physiol. Chem. Phys. **14**, 339 (1982).
[10]P. T. Beall, B. B. Asch, D. C. Chang, D. Medina, and C. F. Hazlewood, J. Natl. Cancer Inst. **64**, 335 (1980).
[11]P. T. Beall, B. B. Asch, D. Medina, and C. Hazlewood, in the *Transformed Cell*, edited by I. L. Cameron and T. B. Pool (Academic, New York, 1981), pp. 293–325.
[12]P. T. Beall and C. F. Hazlewood, in *Nuclear Magnetic Resonance (NMR) Imaging*, edited by C. L. Partain, E. James, and F. D. Rollo (Saunders, Philadelphia, 1983), pp. 312–338.
[13]P. T. Beall, D. Medina, and C. F. Hazlewood, in *NMR in Medicine*, edited by R. Damadian (Springer–Verlag, New York, 1981), pp. 39–57.
[14]P. S. Belton, R. R. Jackson, and K. J. Packer, Biochim. Biophys. Acta **286**, 16 (1972).
[15]G. J. Bene, B. Borcard, V. Graf, E. Hiltbrand, P. Magnin, and F. Naock, Z. Naturforsh. **37**, 394 (1982).
[16]J. A. O. Besson, F. M. Corrigan, E. L. Iljon-Foreman, L. M. Eastwood, F. W. Smith, and G. W. Ashcroft, in *Proceedings of the 2nd Annual Meeting of the Society of Magnetic Resonance in Medicine* (Society of Magnetic Resonance in Medicine, Berkeley, CA, 1983), pp. 43–44.
[17]R. E. Block and G. P. Maxwell, J. Magn. Reson. **14**, 329 (1974).
[18]R. E. Block, G. P. Maxwell, and D. L. Branam, J. Natl. Cancer Inst. **59**, 1731 (1977).
[19]N. Bloembergen, E. M. Purcell, and R. V. Pound, Phys. Rev. **73**, 679 (1948).
[20]C. A. Boicelli, C. Guarnieri, and R. Toni, in *Proceedings of the 2nd Annual Meeting of the Society of Magnetic Resonance in Medicine* (Society of Magnetic Resonance in Medicine, Berkeley, CA, 1983), pp. 47–48.
[21]L. Borghi, F. Savoldi, R. Scelsi, and M. Villa, Exp. Neurol. **81**, 89 (1983).
[22]P. A. Bottomley, H. R. Hart, W. A. Edelstein, J. F. Schenck, L. S. Smith, W. M. Leue, O. M. Mueller, and R. W. Redington, Lancet **2**, 273 (1983).
[23]P. A. Bottomley, H. R. Hart, W. A. Edelstein, J. F. Schenck, L. S. Smith, W. M. Leue, O. M. Mueller, and R. W. Redington, Radiology **150**, 441 (1984).
[24]P. A. Bottomley, T. H. Foster, R. E. Argersinger, and L. M. Pfeifer (in preparation).
[25]W. M. M. J. Bovee, K. W. Getreuer, J. Smidt, and J. Lindeman, J. Natl. Cancer Inst. **61**, 53 (1978).
[26]W. Bovee, P. Huisman, and J. Smidt, J. Natl. Cancer Inst. **52**, 595 (1974).
[27]R. C. Brasch, D. A. London, G. E. Wesbey, T. N. Tozer, D. E. Nitecki, R. D. Williams, J. Doemeny, L. D. Tuck, and D. P. Lallemand, Radiology **147**, 773 (1983).
[28]C. B. Bratton, A. L. Hopkins, and J. W. Weinberg, Science **147**, 738 (1965).
[29]F. S. Buonanno, J. P. Kistler, L. D. De Witt, I. L. Pykett, and T. J. Brady, Neurol. Clinics **1**, 243 (1983).
[30]F. S. Buonanno, I. L. Pykett, T. J. Brady, J. Vielma, C. T. Burt, M. R. Goldman, W. S. Hinshaw, G. M. Pohost, and J. P. Kistler, Stroke **14**, 178 (1983).
[31]F. S. Buonanno, I. L. Pykett, J. Vielma, T. J. Brady, C. T. Burt, M. R. Goldman, J. H. Newhouse, P. F. J. New, W. S. Hinshaw, G. M. Pohost, and J. P. Kistler, in *Proceedings of the International Symposium on NMR Imaging*, edited by R. L. Witcofski, N. Karsaedt, and C. L. Partain (Bowman Gray School of Medicine, Winston–Salem, NC, 1982), pp. 147–157.
[32]G. M. Bydder, R. E. Steiner, I. R. Young, A. S. Hall, D. J. Thomas, J. Marshall, C. A. Pallis, and N. J. Legg, Am. J. Roentgenol. **139**, 215 (1982).
[33]R. Chandra, D. J. Pizzarello, A. F. Keegan, and N. E. Chase, in *Proceedings of the 2nd Annual Meeting of the Society of Magnetic Resonance in Medicine* (Society of Magnetic Resonance in Medicine, Berkeley, CA, 1983), pp. 132–133.
[34]D. C. Chang and C. F. Hazlewood, J. Magn. Reson. **18**, 550 (1975).
[35]D. C. Chang, C. F. Hazlewood, and D. E. Woessner, Biochim. Biophys. Acta **437**, 253 (1976).
[36]R. S. Chaughule, S. F. Kasturi, and S. S. Ranade, Proc. Nucl. Phys. Solid State Phys. Symp. **17C**, 416 (1974).
[37]R. S. Chaughule, S. R. Kasturi, R. Vijayaraghavan, and S. S. Ranade, Ind. J. Biochem. Biophys. **11**, 256 (1974); M. M. Civan and M. Shporer, Biophys. J. **15**, 299 (1975).
[38]B. Coles, J. Natl. Cancer Inst. **57**, 389 (1976).
[39]G. L. Cottam, A. Vasek, and D. Lusted, Res. Commun. Chem. Pathol. Pharmacol. **4**, 495 (1972).
[40]R. Damadian, Science **171**, 1151 (1971).
[41]R. Damadian, K. Zaner, and D. Hor, Physiol. Chem. Phys. **5**, 381 (1973).
[42]R. Damadian, K. Zaner, D. Hor, and T. DiMaio, Proc. Natl. Acad. Sci. **71**, 1471 (1974).
[43]P. L. Davis, L. Kaufman, and L. E. Crooks, in *Proceedings of the International Symposium on NMR Imaging*, edited by R. L. Witcofski, N. Karstaedt, C. L. Partain (Bowman Gray School of Medicine, Winston–Salem, NC, 1982), pp. 101–105.
[44]P. L. Davis, L. Kaufman, L. E. Crooks, and A. R. Margulis, *Nuclear Magnetic Resonance Imaging in Medicine*, edited by R. L. Witcofski, N. Karstaedt, and C. L. Partain (Igaku–Shoin, New York, 1981), pp. 71–100.
[45]P. L. Davis, P. Sheldon, L. Kaufman, L. E. Crooks, A. R. Margulis, J. Miller, J. Watts, M. Arakawa, and J. Hoenninger, Cancer **51**, 433 (1983).
[46]J. D. deCertaines, J. P. Moulinoux, L. Benoist, A. Bernard, and P. Rivet, Life Sci. **31**, 505 (1982).
[47]J. G. Diegel and M. M. Pintar, Biophys. J. **15**, 855 (1975).
[48]G. Diegel and M. M. Pintar, J. Natl. Cancer Inst. **55**, 725 (1975).
[49]F. H. Doyle, J. M. Pennock, L. M. Banks, M. J. McDonnell, G. M. Bydder, R. E. Steiner, I. R. Young, G. J. Clarke, T. Pasmore, and G. Gilderdale, Am. J. Roentgenol. **138**, 193 (1982).
[50]J. S. Economou, L. C. Parks, L. A. Saryan, D. P. Hollis, J. L. Czeisler, and J. C. Eggleston, Surg. Forum **24**, 127 (1973).
[51]W. A. Edelstein, P. A. Bottomley, H. R. Hart, and L. S. Smith, J. Comput. Assist. Tomogr. **7**, 391 (1983).
[52]J. C. Eggleston, L. A. Saryan, and D. P. Hollis, Cancer Res. **35**, 1326 (1975).
[53]S. J. El Yousef, J. P. Lipuma, P. J. Bryan, J. R. Haaga, and R. J. Alfidi, Appl. Radiol. **12**, 65 (1983).
[54]J. M. Escanye, D. Canet, and J. Robert, Biochim. Biophys. Acta **721**, 305 (1982).
[55]J. M. Escanye, D. Canet, J. Robert, and J. Brondeau, Cancer Detection and Prevention **4**, 261 (1981).
[56]J. L. Evelhoch and J. J. H. Ackerman, J. Magn. Reson. **53**, 52 (1983).
[57]E. D. Finch and L. D. Homer, Biophys. J. **14**, 907 (1974).
[58]R. A. Floyd, T. Yoshida, and J. S. Leigh, Jr., Proc. Natl. Acad. Sci. **72**, 56 (1975).
[59]H. E. Frey, R. R. Knispel, J. Kruuv, A. R. Sharp, R. T. Thompson, and M. M. Pintar, J. Natl. Cancer Inst. **49**, 903 (1972).
[60]G. D. Fullerton, J. L. Potter, and N. C. Dornbluth, Magn. Reson. Imag. **1**, 209 (1982).
[61]B. M. Fung, Biochim. Biophys. Acta **497**, 317 (1977).
[62]B. M. Fung, Biophys. J. **18**, 235 (1977).
[63]B. M. Fung, D. L. Durham, and D. A. Wassil, Biochim. Biophys. Acta **399**, 191 (1975).
[64]B. M. Fung, and T. McGaughy, Biochim. Biophys. Acta **343**, 663 (1974).
[65]M. Furuse, K. Saso, Y. Motegi, S. Inao, and A. Izawa, in *Proceedings of the 2nd Annual Meeting of the Society of Magnetic Resonance in Medicine* (Society of Magnetic Resonance in Medicine, Berkeley, CA, 1983), pp. 132–133.
[66]K. J. Go, R. L. Kamman, F. A. J. Muskiet, H. J. C. Berendsen, and P. Van Dijk, in *Proceedings of the 2nd Annual Meeting of the Society of Magnetic Resonance in Medicine* (Society of Magnetic Resonance in Medicine, Berkeley, CA, 1983), pp. 140–141.
[67]M. Goldsmith, J. A. Koutcher, and R. Damadian, Br. J. Cancer **38**, 547 (1978).
[68]M. Goldsmith, J. Koutcher, and R. Damadian, Cancer **41**, 183 (1978).
[69]M. Goldsmith, J. A. Koutcher, and R. Damadian, Br. J. Cancer **36**, 235 (1977).
[70]J. C. Gore, F. H. Doyle, and J. M. Pennock, in *Nuclear Magnetic Resonance Imaging*, edited by C. L. Partain, A. E. James, F. D. Rollo, and R. R. Price (Saunders, Philadelphia, 1983), pp. 94–106.
[71]J. C. Gore, F. H. Doyle, and J. M. Pennock, Proc. Soc. Photo- Opt. Instrum. Eng. **273**, 8 (1981).
[72]W. Von Grodd and W. G. H. Schmitt, Fortschr. Roentgenstr. **139**, 223 (1983).
[73]H. R. Hart, P. A. Bottomley, W. A. Edelstein, S. G. Karr, W. M. Leue, O. M. Mueller, R. W. Redington, J. F. Schenck, L. S. Smith, and D. Vatis, Am. J. Roentgenol. **141**, 1195 (1983).
[74]C. F. Hazlewood, D. C. Chang, D. Medina, G. Cleveland, and B. L.

Nichols, Proc. Natl. Acad. Sci. **69**, 1478 (1972).
[75]C. F. Hazlewood, D. C. Chang, B. L. Nichols, and D. E. Wiessner, Biophys. J. **14**, 583 (1974).
[76]C. F. Hazlewood, G. Cleveland, and D. Medina, J. Natl. Cancer Inst. **52**, 1849 (1974).
[77]C. F. Hazlewood, B. L. Nichols, D. C. Chang, and B. Brown, Johns Hopkins Med. J. **128**, 117 (1971).
[78]G. Held, F. Noack, V. Pollack, and B. Melton, Z. Naturforsch. **28** C, 59 (1973).
[79]M. Heller, K. L. Moon, C. A. Helms, H. Schild, N. I. Chafetz, J. Rodrigo, H. E. Jergesen, and H. K. Genant, in *Proceedings of the 2nd Annual Meeting of the Society Magnetic Resonance in Medicine* (Society Magnetic Resonance in Medicine, Berkeley, CA, 1983), pp. 152–153.
[80]R. Herfkens, P. L. Davis, L. E. Crooks, L. Kaufman, D. Price, T. Miller, A. R. Margulis, J. Watts, J. Hoenninger, M. Arakawa, and R. McRee, Radiology **141**, 211 (1981).
[81]R. J. Herfkens, R. Sievers, L. Kaufman, P. E. Sheldon, D. A. Ortendahl, M. J. Lipton, L. E. Crooks, and C. B. Higgins, Radiology **147**, 749 (1983).
[82]C. B. Higgins, R. Herfkens, M. J. Lipton, R. Sievers, P. Sheldon, L. Kaufman, and L. E. Crooks, Am. J. Cardiol. **52**, 184 (1983).
[83]C. B. Higgins, D. Stark, P. Lanzer, E. H. Botvinick, M. J. Lipton, N. Schiller, R. J. Herfkens, L. Crooks, and L. Kaufman, in *Proceedings of the 2nd Annual Meeting of the Society of Magnetic Resonance in Medicine* (Society of Magnetic Resonance in Medicine, Berkeley, CA, 1983), p. 154.
[84]D. P. Hollis, J. S. Economou, L. C. Parks, J. C. Eggleston, L. A. Saryan, and J. L. Czeisler, Cancer Res. **33**, 2156 (1973).
[85]D. P. Hollis and R. L. Nunnally (private communication, 1976).
[86]D. P. Hollis, L. A. Saryan, J. S. Economon, J. C. Eggleston, J. L. Czeisler, and H. P. Morris, J. Natl. Cancer Inst. **53**, 807 (1974).
[87]D. P. Hollis, L. A. Saryan, J. C. Eggleston, and H. P. Morris, J. Natl. Cancer Inst. **54**, 1469 (1975).
[88]H. Hricak, R. D. Williams, K. L. Moon, A. A. Moss, C. Alpers, L. E. Crooks, and L. Kaufman, Radiology **147**, 765 (1983).
[89]A. Huggert and E. Odelblad, Acta Radiol. **51**, 385 (1958).
[90]J. M. S. Hutchison and F. W. Smith, in *Nuclear Magnetic Resonance Imaging*, edited by C. L. Partain, A. E. James, F. D. Rollo, and R. R. Price (Saunders, Philadelphia, 1983), pp. 231–249.
[91]N. Iijima, S. Saitoo, Y. Yoshida, N. Fujii, T. Koike, K. Osanai, and K. Hirose, Physiol. Chem. Phys. **5**, 431 (1973).
[92]W. R. Inch, J. A. McCredie, R. R. Knispel, R. T. Thompson, and M. M. Pintar, J. Natl. Cancer Inst. **52**, 353 (1974).
[93]M. Jezernick, M. Sentjurc, and M. Schara, Acta Neurochir. **67**, 1 (1983).
[94]S. R. Kasturi, S. S. Ranade, and S. S. Shah, Proc. Indian Acad. Sci. Sect. B. **84**, 60 (1976).
[95]I. C. Kiricuta, Jr., D. Demco, and V. Simplaceanu, Arch. Geschwulstforsh. **42**, 226 (1973).
[96]I. C. Kiricuta, Jr. and V. Simplaceanu, Cancer Res. **35**, 1164 (1975).
[97]I. C. Kiricuta, V. Simplaceanu, and D. Demco, in *Proceedings of the 18th Ampere Congress, Nottingham*, edited by P. S. Allen, E. R. Andrew, and C. A. Bates (North-Holland, Amsterdam, 1975), Vol. I, pp. 287–288.
[98]R. R. Knispel, R. T. Thompson, and M. M. Pintar, J. Magn. Reson. **14**, 44 (1974).
[99]S. H. Koenig, R. D. Brown III, D. Adams, D. Emerson, and C. G. Harrison, IBM Research Report RC 10116 (No. 44807), 1983.
[100]A. Koivula, K. Suominen, T. Timonen, and K. Kiviniitty, Phys. Med. Biol. **27**, 937 (1982).
[101]J. A. Koutcher, M. Goldsmith, and R. Damadian, Cancer **41**, 174 (1978).
[102]C. J. Lewa and Z. Majewska, Bull. Cancer **67**, 525 (1980).
[103]C. J. Lewa and Z. Zbytniewski, Bull. Cancer **63**, 69 (1976).
[104]C. R. Ling and M. A. Foster, Phys. Med. Biol. **27**, 853 (1982).
[105]C. R. Ling, M. A. Foster, and J. M. S. Hutchison, Phys. Med. Biol. **25**, 748 (1980).
[106]C. R. Ling and M. A. Foster, Br. J. Cancer **42**, 148 (1980).
[107]C. R. Ling, M. A. Foster, and J. R. Mallard, Br. J. Cancer **40**, 898 (1979).
[108]C. R. Ling and M. Tucker, J. Natl. Cancer Inst. **64**, 1199 (1980).
[109]J. R. Mallard, J. M. S. Hutchison, W. Edelstein, C. R. Ling, and M. A. Foster, J. Biomed. Eng. **1**, 153 (1979).
[110]I. Mano, R. M. Levy, L. E. Crooks, and Y. Hosobuchi, Invest. Radiol. **17**, 345 (1983).
[111]P. Mansfield and P. G. Morris, *NMR Imaging in Biomedicine* (Academic, New York, 1982), pp. 10–32.
[112]L. A. McLachlan and W. Hamilton, Biochim. Biophys. Acta **583**, 119 (1979).
[113]D. Medina, C. F. Hazlewood, G. G. Cleveland, D. C. Chang, H. J. Spjut, and R. Moyers, J. Natl. Cancer Inst. **54**, 813 (1975).
[114]L. K. Misra, P. A. Narayana, P. T. Beall, S. R. Amtey, and C. F. Hazlewood, in *Proceedings of the 2nd Annual Meeting of the Society of Magnetic Resonance in Medicine* (Society Magnetic Resonance in Medicine, Berkeley, CA, 1983), pp. 264–265.
[115]K. L. Moon, Jr., P. Davis, L. Kaufman, L. E. Crooks, P. E. Sheldon, T. Miller, A. C. Brito, and J. C. Watts, Radiology **148**, 177 (1983).
[116]K. L. Moon, Jr., H. K. Genant, C. A. Helms, N. I. Chafetz, L. E. Crooks, and L. Kaufman, Radiology **147**, 161 (1983).
[117]K. L. Moon, M. Mosley, G. Young, and H. Hricak, in *Proceedings of the 2nd Annual Meeting of the Society of Magnetic Resonance in Medicine* (Society Magnetic Resonance in Medicine, Berkeley, CA, 1983), pp. 245–246.
[118]S. Naruse, Y. Horikawa, C. Tanaka, K. Hirakawa, H. Nishikawa, and K. Yoshizaki, J. Neurosurg. **56**, 747 (1982).
[119]F. Q. H. Ngo, B. J. Glassner, J. W. Bay, A. W. Dudley, and T. F. Meaney, in *Proceedings of the 2nd Annual Meeting of the Society of Magnetic Resonance in Medicine* (Society of Magnetic Resonance in Medicine, Berkeley, CA, 1983), pp. 264–265.
[120]E. Odelblad, Ann. N. Y. Acad. Sci. **82**, 189 (1959).
[121]E. Odelblad, B. N. Bahr, and G. Lindstrom, Arch. Biochem. Biophys. **63**, 221 (1956).
[122]E. Odelblad and U. Bryhn, Acta Radiol. **47**, 315 (1957).
[123]E. Odelblad and G. Lindstrom, Acta Radiol. **43**, 469 (1955).
[124]E. Odelblad and B. Westin, Acta Radiol. **49**, 389 (1958).
[125]D. L. Parker, V. Smith, P. Sheldon, L. E. Crooks, and L. Fussell, Med. Phys. **10**, 321 (1983).
[126]R. G. Parrish, R. J. Kurland, W. W. Janese, and L. Bakay, Science **183**, 438 (1974).
[127]R. T. Pearson, I. D. Duff, W. Derbyshire, and J. M. V. Blanshard, Biochim. Biophys. Acta **362**, 188 (1974).
[128]H. Peemoeller, M. M. Pintar, D. W. Kydon, Biophys. J. **29**, 427 (1980).
[129]J. M. Pennock, Radiography **48**, 221 (1982).
[130]J. F. Polak, R. D. Neirinckx, J. D. Garnic, and D. F. Adams, in *Proceedings of the 2nd Annual Meeting of the Society Magnetic Resonance in Medicine* (Society of Magnetic Resonance in Medicine, Berkeley, CA, 1983), pp. 282–283.
[131]S. S. Ranade, R. S. Chaughule, S. R. Kasturi, J. S. Nadkarni, G. V. Talwalkar, U. V. Wagh, K. S. Korgaonkar, and R. Vijayaraghavan, Ind. J. Biochem. Biophys. **12**, 229 (1975).
[132]S. S. Ranade, S. Shah, S. H. Advani, and S. R. Kasturi, Physiol. Chem. Phys. **9**, 297 (1977).
[133]S. S. Ranade, S. Shah, K. S. Korgaonkar, S. R. Kasturi, R. S. Chaughule, and R. Vijayaraghavan, Physiol. Chem. Phys. **8**, 131 (1976).
[134]S. S. Ranade, S. Shah, R. S. Phadke, and S. R. Kasturi, Physiol. Chem. Phys. **11**, 471 (1979).
[135]S. S. Ranade, S. Shah, and G. V. Talwalkar, Tumori **65**, 157 (1979).
[136]S. Ratkovic and C. Rusov, Period. Biol. **76**, 19 (1974).
[137]A. V. Ratner, E. A. Carter, J. R. Wands, and G. M. Pohost, in *Proceedings of the 2nd Annual Meeting of the Society of Magnetic Resonance in Medicine* (Society Magnetic Resonance in Medicine, Berkeley, CA, 1983), p. 290.
[138]R. J. Ross, J. S. Thompson, K. Kim, and R. A. Bailey, Radiology **143**, 195 (1982).
[139]N. Rupp. M. Reiser, and E. Steller, Eur. J. Radiol. **3**, 68 (1983).
[140]S. N. Rustgi, H. Peemoeller, R. T. Thompson, D. W. Kydon, and M. M. Pintar, Biophys. J. **22**, 439 (1978).
[141]H. S. Sandhu and G. B. Friedmann, Med. Phys. **5**, 514 (1978).
[142]L. A. Saryan, D. P. Hollis, J. S. Economou, and J. C. Eggelston, J. Natl. Cancer Inst. **52**, 599 (1974).
[143]M. Schara, M. Sentjurc, M. Auersperg, and R. Golouh, Br. J. Cancer **29**, 483 (1974).
[144]S. S. Shah, S. S. Ranade, R. S. Phadke, and S. R. Kasturi, Magn. Reson. Imag. **1**, 91 (1982); **1**, 155 (1982).
[145]W. C. Small, M. B. McSweeney, J. H. Goldstein, C. W. Sewell, and R. W. Powell, Biochem. Biophys. Res. Comm. **112**, 991 (1983).
[146]W. C. Small, M. B. McSweeney, M. E. Bernardino, and J. H. Goldstein, in *Proceedings of the 2nd Annual Meeting of the Society of Magnetic Resonance in Medicine* (Society of Magnetic Resonance in Medicine, Berkeley, CA, 1983), pp. 342–343.
[147]F. W. Smith, in *Proceedings of the International Symposium on NMR Imaging*, edited by A. L. Witcofski, N. Karstaedt, and C. L. Partain (Bowman Gray School of Medicine, Winston-Salem, NC, 1982), pp. 125–132.
[148]F. W. Smith, Pediatr. Radiol. **13**, 141 (1983).
[149]F. W. Smith, J. R. Mallard, A. Reid, and J. M. S. Hutchison, Lancet **1**,

963 (1981).
[150]F. W. Smith, A. Reid, J. M. S. Hutchison, and J. R. Mallard, Radiology **142**, 667 (1982).
[151]F. W. Smith, A. Reid, J. R. Mallard, J. M. S. Hutchison, D. A. Power, and G. R. D. Catto, Diagn. Imag. **51**, 209 (1982).
[152]D. D. Stark, N. M. Bass, A. A. Moss, B. R. Bacon, J. H. McKerrow, C. E. Cann, A. Brito, and H. I. Goldberg, Radiology **148**, 743 (1983).
[153]E. O. Stejskal, and J. E. Tanner, J. Chem. Phys. **42**, 288 (1965).
[154]K. Straughan, D. H. Spencer, G. M. Bydder, in *Nuclear Magnetic Resonance Imaging*, edited by C. L. Partain, A. E. James, F. D. Rollo, and R. R. Price (Saunders, Philadelphia, 1983), pp. 195–206.
[155]J. Tennvall, A. Biorklund, T. Moller, M. Olsson, B. Persson, and M. Akerman, in *Proceedings of the 2nd Annual Meeting of the Society of Magnetic Resonance in Medicine* (Society of Magnetic Resonance in Medicine, Berkeley, CA, 1983), pp. 356–357.
[156]D. I. Thickmann, H. L. Kundel, G. Wolf, Radiology **148**, 183 (1983).
[157]F. W. Wehrli, J. R. MacFall, and G. H. Glover, Proc. SPIE **419**, 256 (1983).
[158]G. Wesbey, H. I. Goldberg, J. Mayo, K. Moon, D. Stark, and A. Moss, in *Proceedings of the 2nd Annual Meeting of the Society of Magnetic Resonance in Medicine* (Society of Magnetic Resonance in Medicine, Berkeley, CA, 1983), pp. 373–374.
[159]D. E. Woessner, J. Chem. Phys. **36**, 1 (1962).
[160]G. L. Wolf and L. Baum, Am. J. Roentgenol. **141**, 193 (1983).
[161]G. L. Wolf and B. Conard, Physiol. Chem. Phys. **15**, 19 (1983).
[162]S. H. Koenig, R. D. Brown, D. Adams, D. Emerson, and C. G. Harrison, Invest. Radiol. **19**, 76 (1984).
[163]R. Kimmich, W. Nusser, and F. Winter, Phys. Med. Biol. **29**, 593 (1984).
[164]C. J. G. Bakker and J. Vriend, Phys. Med. Biol. **29**, 509 (1984).
[165]H. T. Edzes and E. T. Samulski, J. Magn. Reson. **31**, 207 (1978).